行政院國家科學委員會專題研究計畫 成果報告

應用非線性時變模式之大型風力機用增速行星齒輪箱承受變動負載之動態響應分析
研究成果報告(精簡版)

計 畫 類 別 ：個別型
計 畫 編 號 ：NSC 99-2221-E-216-003-
執 行 期 間 ：99 年 08 月 01 日至 100 年 10 月 31 日
執 行 單 位 ：中華大學機械工程學系

計 畫 主 持 人：黃國饒

計畫參與人員：碩士班研究生-兼任助理人員：陳冠瑋
碩士班研究生-兼任助理人員：陳頌文
碩士班研究生-兼任助理人員：邱晨熙

報 告 附 件 ：出席國際會議研究心得報告及發表論文

公 開 資 訊 ：本計畫可公開查詢

中 華 民 國 101 年 01 月 30 日

中 文 摘 要 ： 百萬瓦級風力發電機組多需仰賴高可靠度增速百倍多階行星式螺旋齒輪箱或行星式系統搭配平行軸齒輪來達成，因此對於齒輪系統態特性掌握尤為重要。螺旋行星式齒輪箱動態分析為高自由度複雜動態系統，本計畫已完成承受各種變動負載下單級增速螺旋行星式齒輪箱之模態與動態分析方法建立與成果。分別應用非線性時變等效離散動態模式與有限元素連體模式來分析單階齒輪箱之動態響應與振動模態特性。在離散模式方面，完成內/外螺旋齒輪對之非線性時變等效嚙合剛度計算，並考慮齒輪對相位關係以及組裝與幾何關係，此外也推導出可考慮剛體運動效應之單級螺旋行星齒輪系之離散運動方程式，包含軸承、輸出入軸與箱體剛性以及風場與操作資料之輸出入軸的負載變動之考慮，可獲得行星齒輪系統的動態特性以及動態齒輪應力與動態軸承負載，此外進行模態分析計算自然頻率與模態，而非線性嚙合剛度模型則可以討論諧波效應與齒輪動態響應之關係，也以有限元素的動態分析進行初步驗證，未來則將搭配產業實驗結果來驗證非線性時變離散模式分析結果。應用所提出的理論分析模式可以探討各種變動負載下行星式螺旋齒輪箱之暫態與穩態響應特性。本研究已獲得大型風力機用單階行星式螺旋齒輪箱機組包括起動、停機等各種負載運轉條件動態特性的分析技術與成果，若本研究未來得以持續推展，必定可以完成國內大型風力機用增速行星齒輪箱以及如汽車傳動等各種高階齒輪傳動系統的設計分析技術建立。

中文關鍵詞： 行星齒輪系，動態分析，風力發電，有限元素， LS-DYNA

英 文 摘 要 ： To ensure excellent operation of MW-scale wind turbines, high reliable gear boxes adopted for speed increase to one hundred times are the most crucial point which are mostly attained by using the multi-stage planetary systems or compounded with stationary-shaft systems. Among which, well dealing with gear dynamic properties are is rather important topic. Dynamic models of the planetary helical gearings in wind turbines are rather complex and multi degrees of freedom dynamic systems. This study investigates the modal characteristics of single stage planetary gear systems and their dynamic behaviors incorporating fluctuation loading excitations. Two approaches are applied which are an equivalent discrete model and FE model to calculate dynamic responses and modal characteristics,

respectively. In the discrete one, the equivalent time varying mesh stiffness and meshing phases among the external and internal gear pairs have been included. The geometry and assembly constraints of the planetary gear sets are also established. Thus, dynamic equations for single stage planetary helical gearings are derived by incorporating the gross motion effect, also ball bearing and shafts. Fluctuation excitation on input and output shafts is due to wind condition and turbine operation record. Therefore, the dynamic responses of the planetary gear systems are obtained. Their natural frequencies and modal shapes are also resulted. The harmonic effect can be discussed basing on the non linear meshing stiffness. Besides, analyses using an FEM software are used to dynamic analyses of the planetary gear systems. The FE results will be compared with the results of the discrete model. Also, verification using experimental results will be expected via the future collaboration with relating industry enterprises. The effective analysis method and simulating results of single-stage helical planetary gear systems in large scale wind turbines have been obtained by incorporating the fluctuating excitation due to start up and emergency stops, for examples. To found design and analysis techniques of the speed increase in large scale wind turbines not only the higher lever gear transmission of vehicles for example can also be expected by undertaking its future continuous studies.

英文關鍵詞： Planetary gear system, Dynamic analysis, Wind turbine, Finite element, LS-DYNA

行政院國家科學委員會補助專題研究計畫 ■成果報告 □期中進度報告

應用非線性時變模式之大型風力機用增速行星齒輪箱承受變動負載之動態響應分析

計畫類別：■個別型計畫 □整合型計畫
計畫編號：NSC 99 – 2221 – E – 216 - 003
執行期間： 99年8月1日至100年10月31日

執行機構及系所：中華大學機械工程學系

計畫主持人： 黃國饒
共同主持人：
計畫參與人員：陳頌文、陳冠瑋、邱晨熙

成果報告類型(依經費核定清單規定繳交)：■精簡報告 □完整報告

本計畫除繳交成果報告外，另須繳交以下出國心得報告：
□赴國外出差或研習心得報告
□赴大陸地區出差或研習心得報告
■出席國際學術會議心得報告
□國際合作研究計畫國外研究報告

處理方式：除列管計畫及下列情形者外，得立即公開查詢
□涉及專利或其他智慧財產權，□一年□二年後可公開查詢

中 華 民 國 101 年 01 月 31 日

1. 前言

CO2排放與石油枯竭是當前全球最迫切能源環保的兩大課題，各種替代能源開發都受到極大重視。其中以MW級大型風力發電機組之發展最具備經濟成本優勢與潛力，台灣四面環海也具備優越風場條件[1]。目前風力發電機組多朝向發展大型來進行，大型風力發電機風力發電機組造價高達5千萬NTD/MW，運轉壽命需達到20年以上，然而大型風力發電機組運轉，並非如其優雅外觀般平靜，風力機損壞率仍偏高[2]，其中多級增速齒輪系為此等級風力發電機組重要關鍵，為機組中最常出現問題與機組的極脆弱點，且維修點不易到達致維護費用極高，因此增速齒輪箱技術為推展風力發電提昇風力機組運轉可靠度的關鍵。一般齒輪系統終其運轉期間常處於額定負載附近操作，然而風力發電用增速齒輪組，由於風場高度變動與電網安全特性，需考慮起關機、運轉、緊急煞車等變動衝擊負載，容易發生包括齒輪破壞、漏油等，而高速且變動負載激振傳達至軸承更是造成齒輪箱軸承破壞主因，因此掌握增速齒輪箱承受激烈變動負載下的齒輪暫/穩態之動態響應特性，對於提高風力機組系統可靠度極為重要。風力機增速齒輪系統可分為固定軸式與行星軸式兩大類。在MW級風力發電機組設計，為增加扭矩體積比、傳動效率與降低切線速度，幾乎都必須採用行星式而螺旋齒輪系統型式，常採取兩級螺旋行星式齒輪系加上一段固定平行軸式設計[3]或三級都以螺旋行星式齒輪系統[4]的設計，因此完成多級增速螺旋行星式齒輪系統動態特性探討是當前主流研究。本計畫建立單階增速行星齒輪分析方法以有效探討各種負載運轉條件動態特性以完成風力機用齒輪箱分析技術建立。

2.研究目的

行星式螺旋齒輪系統是以行星架結合多個行星齒輪行週轉運動，為複雜之多自由度振動系統。圖1a為典型之 2Z-X形式單級增速螺旋行星齒輪系統。應用計畫申請人近年來所執行計畫所發展承受穩定中等負載之工具機行星齒輪系統之動態分析技術。圖1b為單級的增速螺旋行星齒輪系統之彈簧-阻尼-質量系統之物理模式，先獲得其齒輪對等效時變嚙合剛性，應用拉格蘭吉方程式 (Lagrange's equation)並加以負載與設有，建立離散模式之行星式螺旋齒輪系統運動方程式來分析行星齒輪系模態特性與動態響應。另外以動態有限元素分析軟體LS-DYNA的數值結果之初步驗證離散模式數值結果，未來尋求產學合作，以實驗結果來比較驗證。最後依據風場條件與扭矩變動之關係，探討起動、運轉、關機、緊急煞車等各種緊急情況下暫態與穩態之動態響應，理論模式需能夠考慮各種重要設計參數如齒數搭配、嚙合點、齒輪移位等各種因數之影響。

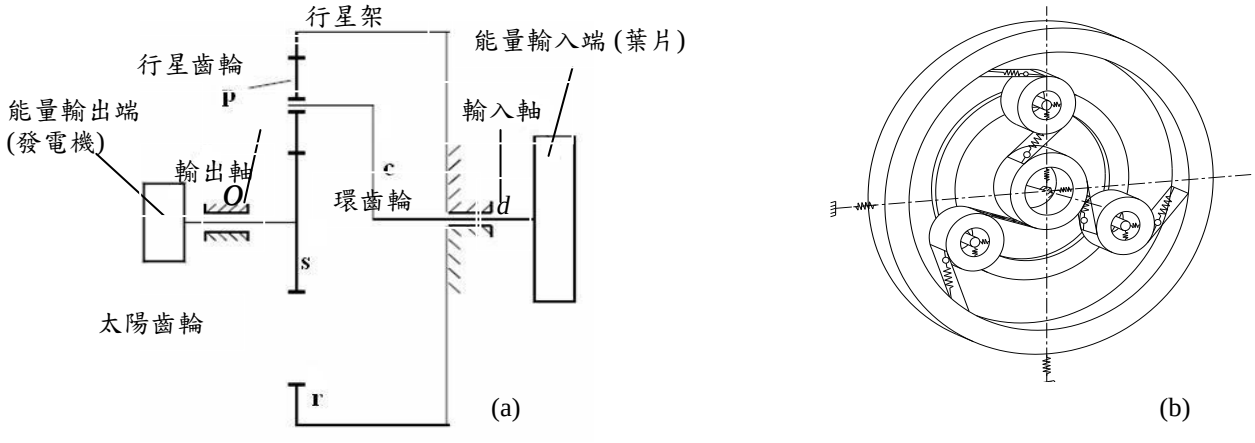

圖2. (a) 2Z-X形式增速行星齒輪系統之構架圖; (b)等效彈簧-質量的離散模式

3.文獻探討

本研究在分析增速螺旋行星式齒輪系動態負荷，以獲得提升大型風力機其運轉安全與壽命的設計技術。一般固定軸螺旋齒輪系的離散模式動態研究文獻發表眾多如 [5,6]且較為完整，而關於以離散模式之螺旋行星齒輪系振動分析為高自由度的系統，其理論模式複雜，影響因素極多如齒數搭配、齒輪嚙合剛性、行星架與軸承剛性以及潤滑條件與阻尼等，本計畫並推導包含嚙合剛性與嚙合相位因素之非線性時變模式之動態分析。關於利用等效離散模式之行星齒輪系動態，August 與Kasuba [7]考慮齒輪對嚙合剛性之變動與太陽齒輪固定方式，對於行星輪齒系統動態力之影響；而Kahraman [8]則改變行星齒輪之個數，考慮齒型誤差造成之激振力，分析行星螺旋齒輪系之振動模態。另根據Velex 和Flamand [9]則指出嚙合齒對剛性對於行星齒輪系較之太陽齒與環齒之支撐剛性影響大。近來關於行星齒輪系統之動態研究，亦開始探討如間隙與磨耗等非線性因素之影響；Sun 和Hu [10]考慮非線性背隙與時變嚙合剛性之行星齒輪系動態特性；Bajer和 Demkowicz [11]則利用多體模式分析行星齒輪系統衝擊能量之變化，而Paker [12]則研究嚙合相位與齒輪系統動態之關係，而最近Ligata等人之研究則開始從事行星齒輪系統實驗，以多位置多個應變規來量測環齒輪的動態齒根應力[13]。大型風機組增速幾乎都採用多級行星式螺旋齒輪箱來達成，而多階行星齒輪系之振動自由度數量與各級齒輪系之幾何與力學相互影響關連更是複雜，因此關於多階行星齒輪系統以離散模式之動態研究則直到最近才開始，[14,15]分析汽車用多階行星齒輪系統之模態特性，而動態響應分析僅進行無相位差線性系統之穩態求解。

由於風力機螺旋增速齒輪箱動態效應產業之振動噪音主要來自於變動負載激振與非線性嚙合剛性之諧波響應所造成，而以離散模式分析變動負載大型增速行星式齒輪系統動態特性與諧波響應研究，則仍未見到。因此本計畫分析單級行星齒輪箱模態與動態特性，探討包括來自於風場條件變動激振、以及非線性齒對嚙合剛性之諧波振動，並尋求產學合作實驗結果與FEM結果來驗證；本計畫可建立承受變動激振負載之單級增速行星式螺旋齒輪箱的動態與模態分析方法與設計技術，並培育高級齒輪與風力發電系統領域設計製造之人才。

4. 研究方法

4.1 理論離散模式

4.1.1 離散模式之行星齒輪系運動方程式推導

應用選擇適當齒輪參數與幾何關係，可組成有/無相位差等間隔或不等間隔之行星齒輪系統，以及各齒輪對之嚙合關係以及時變嚙合剛性，可以改變行星齒輪系統之靜/動態響應特性。而行星齒輪系統之太陽齒輪、行星齒輪和環齒輪之參數選擇需滿足以下條件，其齒輪系統才能成立。

(1) 裝配限制條件

正/螺旋行星齒輪系統中，太陽齒輪、行星齒輪和環齒輪之間的關係須滿足下列三個條件始能順利裝配之。

(i) 中心距同軸條件：各齒輪間之中心距離必須相同，如式(1)。

$$r_p^{\,s} + r_p^{\,p} = r_p^{\,r} - r_p^{\,p} \tag{1}$$

其中 $r_p^{\,s}$ ，$r_p^{\,p}$ ，$r_p^{\,r}$ 分別為太陽齒輪、行星齒輪和環齒輪之節圓半徑長。

(ii) 行星齒輪等分配條件

(a) 行星齒輪成為無相位差之等間隔分配所需條件，為了要讓各行星齒間所夾角度相同，而且為了避免嚙合時太陽齒輪產生徑向負荷所以行星齒輪均勻分佈條件如式(2)。

$$\left(z^s + z^r\right)/N \in I \tag{2}$$

上式中 若 $z^s/N \in I$，則等分行星齒輪系且各行星齒輪與太陽齒輪或環齒輪之嚙合無相位差。

(b) 若行星齒輪為具有相位差之等間隔分配則須滿足式(3)。

$$\left(z^s + z^r\right)\theta/180 \in I \tag{3}$$

z^s、z^r 為太陽齒輪與環齒輪之齒數，N為行星齒的個數，I 表示整數，θ 為相鄰兩行星齒間所成角度的一半。

(c) 若 (2)與(3)式皆無法滿足，行星齒輪系統必為不等間隔分配。

(iii) 避免行星齒輪相碰撞條件: 為了避免相鄰之行星齒輪相碰之條件，行星齒輪間中心距必須大於行星齒頂直徑，若 h_a^p 為行星齒輪齒冠高，z^p 為行星齒輪之齒數，則如式 (4)

$$z^p + 2h_a^p < \left(z^s + z^p\right)\sin(180^o/N) \tag{4}$$

(2) 齒輪對相位差

齒輪對不連續時變嚙合剛性，造成非線性行星齒輪系統之諧波振動，而調整齒輪對相位關係可以改變此非線性特性，並藉此改善其諧波振動現象。圖2(a)表示齒輪對間相位關係。根據行星齒輪系統之齒數搭配 (z^s, z^p, z^r)、行星齒輪數目與 嚙合相位 $\theta_p^{(k)}$，行星齒輪系統於嚙合時第 i 個行星齒輪與其他 $N-1$個行星齒輪與太陽齒輪或環齒輪之嚙合相位有下述關係：(i) 當 z^s/N 與 z^r/N 為整數且行星齒輪等分裝配時，每個行星齒輪之嚙合相位相同，無嚙合相位差；(ii) 當 (i)不成立即 z^s/N 與 z^r/N 不為整數或者行星齒輪以非等分裝配時，如圖2(b)所示，第k個行星齒輪與第1個行星齒輪相隔 $\psi_c^{(k)}$ 角度再自轉 $\Delta\theta_p^{(k)}$ 角度後，第k個行星齒輪得以順利裝配之。$\Delta\theta_p^{(k)}$ 計算如式 (5) [16]

$$\Delta\theta_p^{(k)} = \left(z^s - Int\left(z^s \Big/ \left(2\pi/\psi_c^{(k)}\right)\right)\times\left(2\pi/\psi_c^{(k)}\right)\right) \Big/ \left(2\pi/\psi_c^{(k)}\right)\times\left(2\pi/z^p\right) \tag{5}$$

另外，各種齒輪對嚙合相位之間的關係共分三種：(a)第 k 組外齒輪對與第 1 組外齒輪對間之相位差，(b)第 k 組內齒輪對與第 1 組內齒輪對間之相位差，(c)第 1 組內齒輪對與第 1 組外齒輪對間之相位差。最後應用上述三種齒輪對之相位差關係

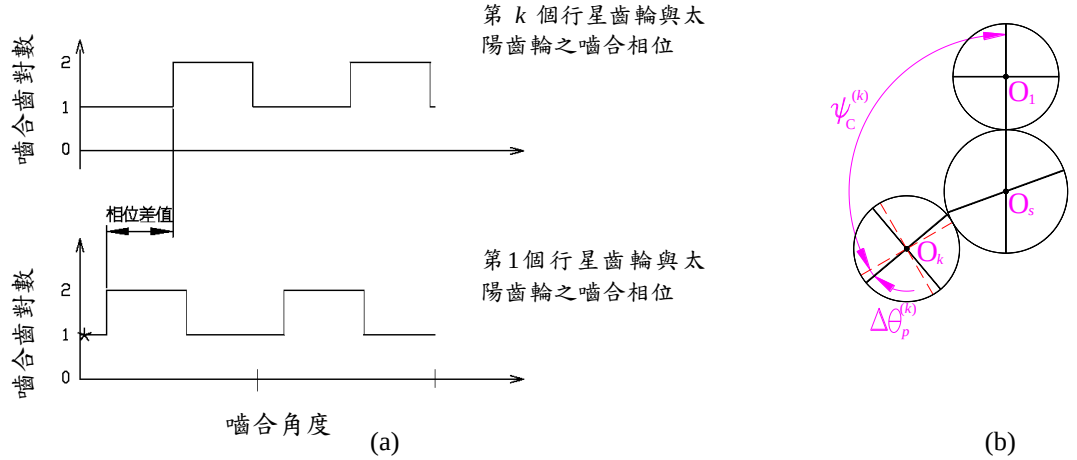

圖2. (a)第k組與第1組齒輪對之嚙合相位差; (b)第k個與第1個行星齒裝配關係圖

(3) 螺旋齒輪對之時變嚙合剛性

應用彈簧-質量的離散模式的行星齒輪動態分析方法需先計算等效太陽齒輪-行星齒輪外齒輪對(圖 3a)與行星齒輪-環齒之內齒輪對(圖 3b)時變嚙合剛度。考慮齒輪系運轉之時變特性以及設計種參數參 數如壓力角、齒數搭配、嚙合點、移位係數等，計算其瞬間嚙合齒對數目與嚙合點位置，以得螺旋齒輪對的等效時變嚙合剛度。

(i)外正齒輪之齒對剛度

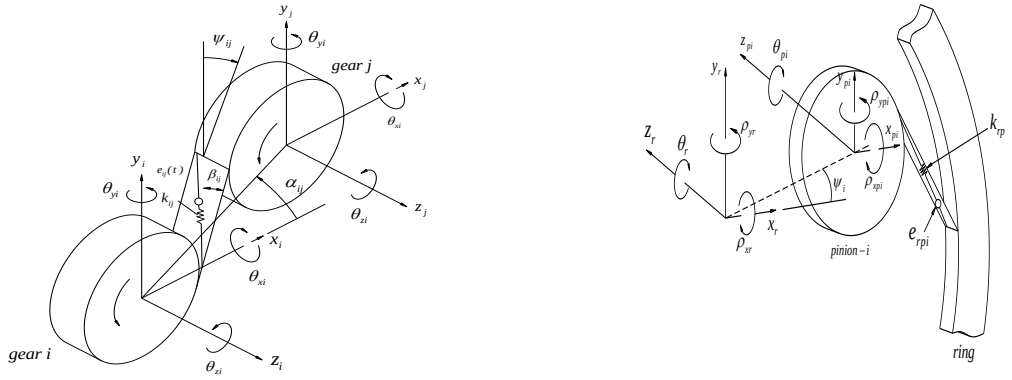

圖3. 外、內螺旋齒輪對的之等效彈簧-質量的離散分析模式

推導外正齒輪對時變等效嚙合剛度，整合齒對嚙合時之赫茲接觸變形、輪齒懸臂樑撓曲變形、本體支撐變形之考慮，因此每單位齒寬之外正齒輪之齒對剛度計算如下

$$k_{gi} = W/(q_{TP} + q_{BP} + q_{TG} + q_{BG} + q_H) \tag{6}$$

上式中 q_{Ti} 、 q_{Bi} 與 q_{Hi} 為各部份之可撓度(compliance)分別為: (1) 輪齒以非均勻截面之樑元素受彎矩、剪力與壓負荷之可撓度。(2) 輪齒與本體彈性支承局部變形之可撓度。(3)嚙合齒對以赫茲接觸瞬間接觸變形之可撓度。單位齒寬之外正齒輪之齒對剛度

然後外螺旋齒輪對等效嚙合剛性計算是以等效正齒輪嚙合剛性來獲得。螺旋齒輪的齒數為z，將以齒數 z' 之正齒輪來等效之，兩個齒數關係可以應用下式獲得

$$z' = z/\cos^3\beta \tag{7}$$

上式中 β 則為螺旋角。在齒輪對運轉過程其嚙合齒對數目(n_{tp})、嚙合齒線長度(L_i)、以及嚙合點位置隨轉動角度變動而有不同，因此其齒輪對嚙合隨轉動角度改變，即為嚙合齒輪對之等效時變剛性。 某一瞬間轉動角度之外螺旋齒輪對(external gear pair)之等效剛性計算如下

$$k_e = \sum_{i=1}^{n_{tp}} k_{e,i} \tag{8}$$

上式中 n_{tp} 為外螺旋齒輪對之瞬間嚙合齒對數目， $k_{e,i}$ 為第 i 外嚙合齒對之等效時變嚙合剛性

$$k_{e,i} = \int_0^{L_i} k_{ei,j} \cdot dL_{i,j} \tag{9}$$

其中 $k_{ei,j}$ 為 第i對之外嚙合齒對之於j嚙合角度之每單位接觸線長的等效法向時變法向嚙合剛性， L_i 第 i 外嚙合齒對之實際接觸線長度，另內螺旋齒輪對可以相似計算過程來獲得。

(4) 離散模式之模態分析與動態求解

包含剛體運動自由度之單級螺旋行星齒輪系離散模式的動態方程式(10)可表示於下

$$\mathbf{M}_1\ddot{\mathbf{X}}_1 + \mathbf{C}_1\dot{\mathbf{X}}_1 + \mathbf{K}_1\mathbf{X}_1 = \mathbf{F}_1 \tag{10}$$

式(10)的下標**1**代表是單一級行星齒輪系統，因此單級行星齒輪系之位移向量 $\mathbf{X}_1$ 是

$$\mathbf{X}_1 = \begin{bmatrix} \mathbf{x}_s & \mathbf{x}_r & \mathbf{x}_1 & \mathbf{x}_2 & .... & \mathbf{x}_{n_p} & \mathbf{x}_c & \mathbf{x}_R \end{bmatrix} \tag{11}$$

將彈性變形自由度與剛體運動自由度分開表示，則可表為

$$\begin{bmatrix} \mathbf{M}_{ff} & \mathbf{M}_{fR} \\ \mathbf{M}_{Rf} & \mathbf{M}_{RR} \end{bmatrix} \begin{bmatrix} \ddot{\mathbf{X}}_f \\ \ddot{\mathbf{X}}_R \end{bmatrix} + \begin{bmatrix} \mathbf{C}_{ff} & 0 \\ 0 & 0 \end{bmatrix} \begin{bmatrix} \dot{\mathbf{X}}_f \\ \dot{\mathbf{X}}_R \end{bmatrix} + \begin{bmatrix} \mathbf{K}_{ff} & 0 \\ 0 & 0 \end{bmatrix} \begin{bmatrix} \mathbf{X}_f \\ \mathbf{X}_R \end{bmatrix} = \begin{bmatrix} \mathbf{F}_f \\ \mathbf{F}_R \end{bmatrix} \tag{12}$$

式(12)中 $\mathbf{X}_f$:彈性變形向量、 $\mathbf{X}_R$:剛體運動自由度位移向量、 $\mathbf{M}_{ij}$:質量矩陣、 $\mathbf{C}_{ff}$:阻尼矩陣、 $\mathbf{K}_{ff}$:剛度矩陣、 $\mathbf{F}_f$:屬於靜力平衡之外力向量、 $\mathbf{F}_R$:屬於造成加速度之外力向量。以下簡述 $\mathbf{K}_{ff}$ 的構成，一個包含 n_p 個行星輪的單級行星齒輪系螺旋之組合剛性矩陣 $\mathbf{K}_{ff}$ 可寫成(13)式

$$\mathbf{K}_{ff}=\begin{bmatrix}\sum_{j}^{n_p}\mathbf{k}_{sj} & -\mathbf{k}_{sj} & \cdots & -\mathbf{k}_{sn_p} & \mathbf{0} & \mathbf{0}\\ & (\mathbf{k}_{s1}+\mathbf{k}_{r1}+\mathbf{k}_{c221}) & \cdots & \mathbf{0} & -\mathbf{k}_{r1} & \mathbf{k}_{c121}\\ & & \ddots & \vdots & \vdots & \vdots\\ & & & (\mathbf{k}_{sn_p}+\mathbf{k}_{rn_p}+\mathbf{k}_{c22n_p}) & -\mathbf{k}_{rn_p} & \mathbf{k}_{c12n_p}\\ & & & & \sum_{j}^{n_p}\mathbf{k}_{sj} & \mathbf{0}\\ & \text{Sym.} & & & & \sum_{j}^{n_p}\mathbf{k}_{c11j}\end{bmatrix} \tag{13}$$

上式中$\mathbf{k}_{*\#}$為6×6的剛性矩陣，下標 *, # 表示 s, r, c, j 分別為太陽齒輪、環形齒輪、行星架、與第j個行星齒輪。本計畫所進行之行星齒輪系非線性時變剛性矩陣推導，是先獲得外齒輪對(圖3a)與內齒輪對(圖3b)單獨齒輪對之等效時變嚙合剛度矩陣。然後應用各個齒輪對剛度矩陣建立，可以極具彈性的組合成各種形式行星齒輪系統之動態方程式。舉例說明之，第(14)式即為所推導之太陽齒輪-行星齒輪單個外齒輪對(圖3a)之12×12剛度矩陣$\mathbf{K}_{sj}$；第(15)式為環齒輪-行星齒輪單個內齒輪對(圖3b)之12×12剛度矩陣$\mathbf{K}_{rj}$，其中$k_{sj}(t)$、$k_{rj}(t)$即為圖1(b)中太陽/環齒輪與第j個行星齒輪間之外、內螺旋齒輪對非線性時變嚙合剛度。

$$\mathbf{K}_{sj}=k_{sj}(t)\begin{bmatrix}
c^2\beta s^2\psi_{sj} & c^2\beta c\psi_{sj}s\psi_{sj} & -c\beta s\beta s\psi_{sj} & c\beta s\beta s^2\psi_{sj} & c\beta s\beta c\psi_{sj}s\psi_{sj} & c^2\beta s\psi_{sj} & -c^2\beta s^2\psi_{sj} & -c^2\beta c\psi_{sj}s\psi_{sj} & c\beta s\beta s\psi_{sj} & c\beta s\beta s^2\psi_{sj} & c\beta s\beta c\psi_{sj}s\psi_{sj} & -c^2\beta s\psi_{sj}\\
c^2\beta c\psi_{sj}s\psi_{sj} & c^2\beta c^2\psi_{sj} & -c\beta s\beta c\psi_{sj} & c\beta s\beta c\psi_{sj}s\psi_{sj} & c\beta s\beta c^2\psi_{sj} & c^2\beta c\psi_{sj} & -c^2\beta c\psi_{sj}s\psi_{sj} & -c^2\beta c^2\psi_{sj} & c\beta s\beta c\psi_{sj} & c\beta s\beta c\psi_{sj}s\psi_{sj} & c\beta s\beta c^2\psi_{sj} & -c^2\beta c\psi_{sj}\\
-c\beta s\beta s\psi_{sj} & -c\beta s\beta c\psi_{sj} & s^2\beta & -s^2\beta s\psi_{sj} & -s^2\beta c\psi_{si} & -c\beta s\beta & c\beta s\beta s\psi_{sj} & c\beta s\beta c\psi_{sj} & -s^2\beta & -s^2\beta s\psi_{sj} & -s^2\beta c\psi_{si} & c\beta s\beta\\
c\beta s\beta s^2\psi_{sj} & c\beta s\beta c\psi_{sj}s\psi_{sj} & -s^2\beta s\psi_{sj} & s^2\beta s^2\psi_{sj} & s^2\beta c\psi_{si}s\psi_{sj} & c\beta s\beta s\psi_{sj} & -c\beta s\beta s^2\psi_{sj} & -c\beta s\beta c\psi_{sj}s\psi_{sj} & s^2\beta s\psi_{sj} & s^2\beta s^2\psi_{sj} & s^2\beta c\psi_{si}s\psi_{sj} & -c\beta s\beta s\psi_{sj}\\
c\beta s\beta c\psi_{sj}s\psi_{sj} & c\beta s\beta c^2\psi_{sj} & -s^2\beta c\psi_{si} & s^2\beta c\psi_{sj}s\psi_{sj} & s^2\beta c^2\psi_{sj} & c\beta s\beta c\psi_{sj} & -c\beta s\beta c\psi_{sj}s\psi_{sj} & -c\beta s\beta c^2\psi_{sj} & s^2\beta c\psi_{si} & s^2\beta c\psi_{si}s\psi_{sj} & s^2\beta c^2\psi_{sj} & -c\beta s\beta c\psi_{sj}\\
c^2\beta s\psi_{sj} & c^2\beta c\psi_{sj} & -c\beta s\beta & c\beta s\beta s\psi_{sj} & c\beta s\beta c\psi_{sj} & c^2\beta & -c^2\beta s\psi_{sj} & -c^2\beta c\psi_{sj} & c\beta s\beta & c\beta s\beta s\psi_{sj} & c\beta s\beta c\psi_{sj} & -c^2\beta\\
-c^2\beta s^2\psi_{sj} & -c^2\beta c\psi_{sj}s\psi_{sj} & c\beta s\beta s\psi_{sj} & -c\beta s\beta s^2\psi_{sj} & -c\beta s\beta c\psi_{sj}s\psi_{sj} & -c^2\beta s\psi_{sj} & c^2\beta s^2\psi_{sj} & c^2\beta c\psi_{sj}s\psi_{sj} & -c\beta s\beta s\psi_{sj} & -c\beta s\beta s^2\psi_{sj} & -c\beta s\beta c\psi_{sj}s\psi_{sj} & c^2\beta s\psi_{sj}\\
-c^2\beta c\psi_{sj}s\psi_{sj} & -c^2\beta c^2\psi_{sj} & c\beta s\beta c\psi_{sj} & -c\beta s\beta c\psi_{sj}s\psi_{sj} & -c\beta s\beta c^2\psi_{sj} & -c^2\beta c\psi_{sj} & c^2\beta c\psi_{sj}s\psi_{sj} & c^2\beta c^2\psi_{sj} & -c\beta s\beta c\psi_{sj} & -c\beta s\beta c\psi_{sj}s\psi_{sj} & -c\beta s\beta c^2\psi_{sj} & c^2\beta c\psi_{sj}\\
c\beta s\beta s\psi_{sj} & c\beta s\beta c\psi_{sj} & -s^2\beta & s^2\beta s\psi_{sj} & s^2\beta c\psi_{si} & c\beta s\beta & -c\beta s\beta s\psi_{sj} & -c\beta s\beta c\psi_{sj} & s^2\beta & s^2\beta s\psi_{sj} & s^2\beta c\psi_{si} & -c\beta s\beta\\
c\beta s\beta s^2\psi_{sj} & c\beta s\beta c\psi_{sj}s\psi_{sj} & -s^2\beta s\psi_{sj} & s^2\beta s^2\psi_{sj} & s^2\beta c\psi_{si}s\psi_{sj} & c\beta s\beta s\psi_{sj} & -c\beta s\beta s^2\psi_{sj} & -c\beta s\beta c\psi_{sj}s\psi_{sj} & s^2\beta s\psi_{sj} & s^2\beta s^2\psi_{sj} & s^2\beta c\psi_{si}s\psi_{sj} & -c\beta s\beta s\psi_{sj}\\
c\beta s\beta c\psi_{sj}s\psi_{sj} & c\beta s\beta c^2\psi_{sj} & -s^2\beta c\psi_{si} & s^2\beta c\psi_{sj}s\psi_{sj} & s^2\beta c^2\psi_{sj} & c\beta s\beta c\psi_{sj} & -c\beta s\beta c\psi_{sj}s\psi_{sj} & -c\beta s\beta c^2\psi_{sj} & s^2\beta c\psi_{si} & s^2\beta c\psi_{si}s\psi_{sj} & s^2\beta c^2\psi_{sj} & -c\beta s\beta c\psi_{sj}\\
-c^2\beta s\psi_{sj} & -c^2\beta c\psi_{sj} & c\beta s\beta & -c\beta s\beta s\psi_{sj} & -c\beta s\beta c\psi_{sj} & -c^2\beta & c^2\beta s\psi_{sj} & c^2\beta c\psi_{sj} & -c\beta s\beta & -c\beta s\beta s\psi_{sj} & -c\beta s\beta c\psi_{sj} & c^2\beta
\end{bmatrix} \tag{14}$$

$$\mathbf{K}_{rj}=k_{rj}(t)\begin{bmatrix}
c^2\beta s^2\psi_{rj} & -c^2\beta c\psi_{rj}s\psi_{rj} & -c\beta s\beta s\psi_{rj} & c\beta s\beta s^2\psi_{rj} & c\beta s\beta c\psi_{rj}s\psi_{rj} & c^2\beta s\psi_{rj} & -c^2\beta s^2\psi_{rj} & c^2\beta c\psi_{rj}s\psi_{rj} & c\beta s\beta s\psi_{rj} & c\beta s\beta s^2\psi_{rj} & -c\beta s\beta c\psi_{rj}s\psi_{rj} & -c^2\beta s\psi_{rj}\\
-c^2\beta c\psi_{rj}s\psi_{rj} & c^2\beta c^2\psi_{rj} & c\beta s\beta c\psi_{rj} & -c\beta s\beta c\psi_{rj}s\psi_{rj} & -c\beta s\beta c^2\psi_{rj} & -c^2\beta c\psi_{rj} & c^2\beta c\psi_{rj}s\psi_{rj} & -c^2\beta c^2\psi_{rj} & -c\beta s\beta c\psi_{rj} & -c\beta s\beta c\psi_{rj}s\psi_{rj} & c\beta s\beta c^2\psi_{rj} & c^2\beta c\psi_{rj}\\
-c\beta s\beta s\psi_{rj} & c\beta s\beta c\psi_{rj} & s^2\beta & -s^2\beta s\psi_{rj} & -s^2\beta c\psi_{rj} & -c\beta s\beta & c\beta s\beta s\psi_{rj} & -c\beta s\beta c\psi_{rj} & -s^2\beta & -s^2\beta s\psi_{rj} & s^2\beta c\psi_{rj} & c\beta s\beta\\
c\beta s\beta s^2\psi_{rj} & -c\beta s\beta c\psi_{rj}s\psi_{rj} & -s^2\beta s\psi_{rj} & s^2\beta s^2\psi_{rj} & s^2\beta c\psi_{rj}s\psi_{rj} & c\beta s\beta s\psi_{rj} & -c\beta s\beta s^2\psi_{rj} & c\beta s\beta c\psi_{rj}s\psi_{rj} & s^2\beta s\psi_{rj} & s^2\beta s^2\psi_{rj} & -s^2\beta c\psi_{rj}s\psi_{rj} & -c\beta s\beta s\psi_{rj}\\
c\beta s\beta c\psi_{rj}s\psi_{rj} & -c\beta s\beta c^2\psi_{rj} & -s^2\beta c\psi_{rj} & s^2\beta c\psi_{rj}s\psi_{rj} & s^2\beta c^2\psi_{rj} & c\beta s\beta c\psi_{rj} & -c\beta s\beta c\psi_{rj}s\psi_{rj} & c\beta s\beta c^2\psi_{rj} & s^2\beta c\psi_{rj} & s^2\beta c\psi_{rj}s\psi_{rj} & -s^2\beta c^2\psi_{rj} & -c\beta s\beta c\psi_{rj}\\
c^2\beta s\psi_{rj} & -c^2\beta c\psi_{rj} & -c\beta s\beta & c\beta s\beta s\psi_{rj} & c\beta s\beta c\psi_{rj} & c^2\beta & -c^2\beta s\psi_{rj} & c^2\beta c\psi_{rj} & c\beta s\beta & c\beta s\beta s\psi_{rj} & -c\beta s\beta c\psi_{rj} & -c^2\beta\\
-c^2\beta s^2\psi_{rj} & c^2\beta c\psi_{rj}s\psi_{rj} & c\beta s\beta s\psi_{rj} & -c\beta s\beta s^2\psi_{rj} & -c\beta s\beta c\psi_{rj}s\psi_{rj} & -c^2\beta s\psi_{rj} & c^2\beta s^2\psi_{rj} & -c^2\beta c\psi_{rj}s\psi_{rj} & -c\beta s\beta s\psi_{rj} & -c\beta s\beta s^2\psi_{rj} & c\beta s\beta c\psi_{rj}s\psi_{rj} & c^2\beta s\psi_{rj}\\
c^2\beta c\psi_{rj}s\psi_{rj} & -c^2\beta c^2\psi_{rj} & -c\beta s\beta c\psi_{rj} & c\beta s\beta c\psi_{rj}s\psi_{rj} & c\beta s\beta c^2\psi_{rj} & c^2\beta c\psi_{rj} & -c^2\beta c\psi_{rj}s\psi_{rj} & c^2\beta c^2\psi_{rj} & c\beta s\beta c\psi_{rj} & c\beta s\beta c\psi_{rj}s\psi_{rj} & -c\beta s\beta c^2\psi_{rj} & -c^2\beta c\psi_{rj}\\
c\beta s\beta s\psi_{rj} & -c\beta s\beta c\psi_{rj} & -s^2\beta & s^2\beta s\psi_{rj} & s^2\beta c\psi_{rj} & c\beta s\beta & -c\beta s\beta s\psi_{rj} & c\beta s\beta c\psi_{rj} & s^2\beta & s^2\beta s\psi_{rj} & -s^2\beta c\psi_{rj} & -c\beta s\beta\\
c\beta s\beta s^2\psi_{rj} & -c\beta s\beta c\psi_{rj}s\psi_{rj} & -s^2\beta s\psi_{rj} & s^2\beta s^2\psi_{rj} & s^2\beta c\psi_{rj}s\psi_{rj} & c\beta s\beta s\psi_{rj} & -c\beta s\beta s^2\psi_{rj} & c\beta s\beta c\psi_{rj}s\psi_{rj} & s^2\beta s\psi_{rj} & s^2\beta s^2\psi_{rj} & -s^2\beta c\psi_{rj}s\psi_{rj} & -c\beta s\beta s\psi_{rj}\\
-c\beta s\beta c\psi_{rj}s\psi_{rj} & c\beta s\beta c^2\psi_{rj} & s^2\beta c\psi_{rj} & -s^2\beta c\psi_{rj}s\psi_{rj} & -s^2\beta c^2\psi_{rj} & -c\beta s\beta c\psi_{rj} & c\beta s\beta c\psi_{rj}s\psi_{rj} & -c\beta s\beta c^2\psi_{rj} & -s^2\beta c\psi_{rj} & -s^2\beta c\psi_{rj}s\psi_{rj} & s^2\beta c^2\psi_{rj} & c\beta s\beta c\psi_{rj}\\
-c^2\beta s\psi_{rj} & c^2\beta c\psi_{rj} & c\beta s\beta & -c\beta s\beta s\psi_{rj} & -c\beta s\beta c\psi_{rj} & -c^2\beta & c^2\beta s\psi_{rj} & -c^2\beta c\psi_{rj} & -c\beta s\beta & -c\beta s\beta s\psi_{rj} & c\beta s\beta c\psi_{rj} & c^2\beta
\end{bmatrix} \tag{15}$$

(5) 模態型式與模態動態求解

本研究分別進行3D行星齒輪系模態分析與動態響應求解。根據Parker等人之研究[12]，將其2D系統振動模態歸納為平移模態、旋轉模態、行星模態三類，如圖4所示。若行星齒輪系統為無相位差之等間隔分配時，其平移模態下，其太陽齒輪、行星架與環齒輪呈現相互直

交的兩種平移位移模式，故平移模態的頻率重複數為2。行星模態之頻率則重複$N-3$次，N表行星齒輪個數；當行星齒輪個數為4時，頻率重複數為1，此時行星模態之行星齒輪僅一種位移模式，而行星齒輪個數為5時，各組行星模態之行星齒輪則有兩種位移模式，

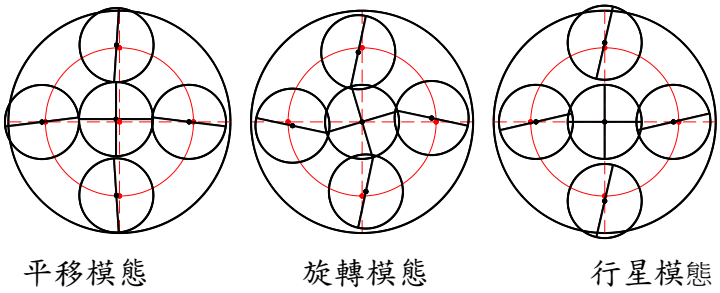

圖4. 2D離散模式之行星齒輪系三種模態型式

接下來說明考慮剛體運動自由度之單級螺旋行星齒輪系離散模式動態響應分析過程如下，

$$\mathbf{M}_{ff}\ddot{\mathbf{X}}_f+\mathbf{M}_{fR}\ddot{\mathbf{X}}_R+\mathbf{C}_{ff}\dot{\mathbf{X}}_f+\mathbf{K}_{ff}\mathbf{X}_f=\mathbf{F}_f \tag{16}$$

$$\mathbf{M}_{Rf}\ddot{\mathbf{X}}_f+\mathbf{M}_{RR}\ddot{\mathbf{X}}_R=\mathbf{F}_R \tag{17}$$

(i)若邊界條件為剛體加速度激振條件，即$\ddot{\mathbf{X}}_R$已知，則可以由直接(16)式以數值積分求解彈性變形向量$\mathbf{X}_f$；(ii) 若邊界條件為加速度外力邊界條件，即$\mathbf{F}_R$已知，則由從(17)式

$$\ddot{\mathbf{X}}_R=\mathbf{M}_{RR}^{-1}(\mathbf{F}_2-\mathbf{M}_{Rf}\ddot{\mathbf{X}}_f) \tag{18}$$

將(18)式代回(16)式

$$(\mathbf{M}_{ff}-\mathbf{M}_{fR}\mathbf{M}_{RR}^{-1}\mathbf{M}_{Rf})\ddot{\mathbf{X}}_f+\mathbf{C}_{ff}\dot{\mathbf{X}}_f+\mathbf{K}_{ff}\mathbf{X}_f=\mathbf{F}_f-\mathbf{M}_{fR}\mathbf{M}_{RR}^{-1}\mathbf{F}_R \tag{19}$$

同樣的可以以數值積分求解出彈性變形向量$\mathbf{X}_f$，以下結果以剛體加速度條件進行求解。

(6) 以FEM與實驗結果比較驗證

本研究理論分析數值結果希望以實驗結果驗證之，但由於大型行星齒輪系動態實驗所需之齒輪模組製作與量測設備所需經費龐大高達千萬元。先應用有限元素分析軟體LS-DYNA之數值計算結果，進行初步比較，圖5a即為行星齒輪系統之FEM分析網格。目前已與行星齒輪系製造與大型風力機廠商搭配，未來可以實驗來驗證之[13]。圖5b、c為應用LS-DYNA之FEM分析大型行星齒輪系之動態與模態結果範例圖示。

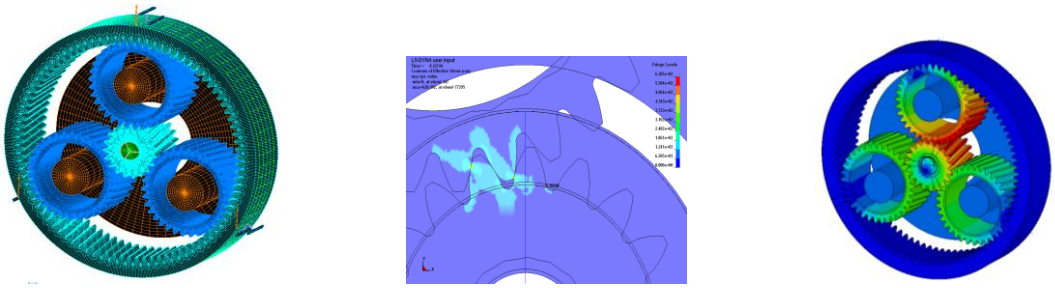

(a) 3D網格模式　　(b) 動態響應　　(c) 模態響應

圖 5. 應用LS-DYNA分析3D行星齒輪系動/模態分析的網格模式與結果

5. 結果與討論

5.1 分析模式與螺旋齒輪對嚙合剛度

圖6a所示為一風力機主力機種增速齒輪箱之第一級的3個螺旋行星齒輪大形單階行星齒輪系(19-34- 89)三D等效離散模式，其FE連體模式於圖5a，齒輪箱傳遞功率為2.2MW，風力機運

轉切入風速約為 3.5m/s (3級風)、額定風速約12m/s、切斷風速約為 25m/s (9級風)，基本數據: 法向模數=16mm，其太陽、行星與環齒輪齒數分別為19、34、89齒，法向壓力角=20°、螺旋角=7°，圖6b為以(9)式所獲得之內外齒輪對的非線性時變嚙合剛度，另外等效軸承剛性向量設定為$\left[k_x \quad k_y \quad k_z \quad k_{x\theta} \quad k_{y\theta} \quad k_{z\theta}\right]=10^{10}\times\left[1 \quad 1 \quad 10 \quad 0.001 \quad 0.001 \quad 0\right]$，其中平移剛性單位為 N/m、旋轉剛性單位為 Nm/rad。

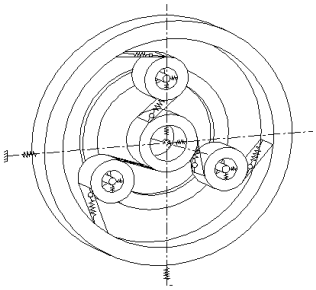

(a)

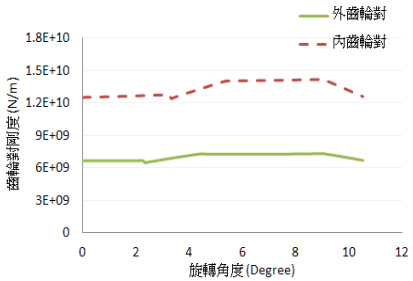

(b)

圖6. 風力機螺旋行星齒輪系(2.2MW): (a) 3D離散模式;(b) 內外齒對非線性時變嚙合剛度

5.2 模態分析結果與比較

應用FEM分析螺旋行星齒輪系（19-34-89）之自然頻率與模態特結果如表1，模態型式範例如圖7所示，定義Z_i為軸向模態、C_i為行星架模態，結果顯示3D模型與2D模型一樣會有16個平面結構模態，包含13個平移模態、3個旋轉模態，另外則出現5個軸向模態，其分為1個太陽齒輪、3個行星齒輪、1個環齒輪軸向模態。

表1．螺旋行星齒輪系自然頻率與模態

模態型式	自然頻率 (Hz)
平移模態 T_i	76.8、77.5、133.4、144.1、222.5、227.1、 272.3、281.2、329.0、1285.3、1328.8、1395.2 、 1665.0
旋轉模態 R_i	130.9、1200.5、2239.5
行星模態 P_i	無 (因行星齒輪個數為3)
行星架模態 C_i	1428.5、1744.1、1744.2
軸向模態 Z_i	714.5、1446.1、1456.9、1502.2、1546.9

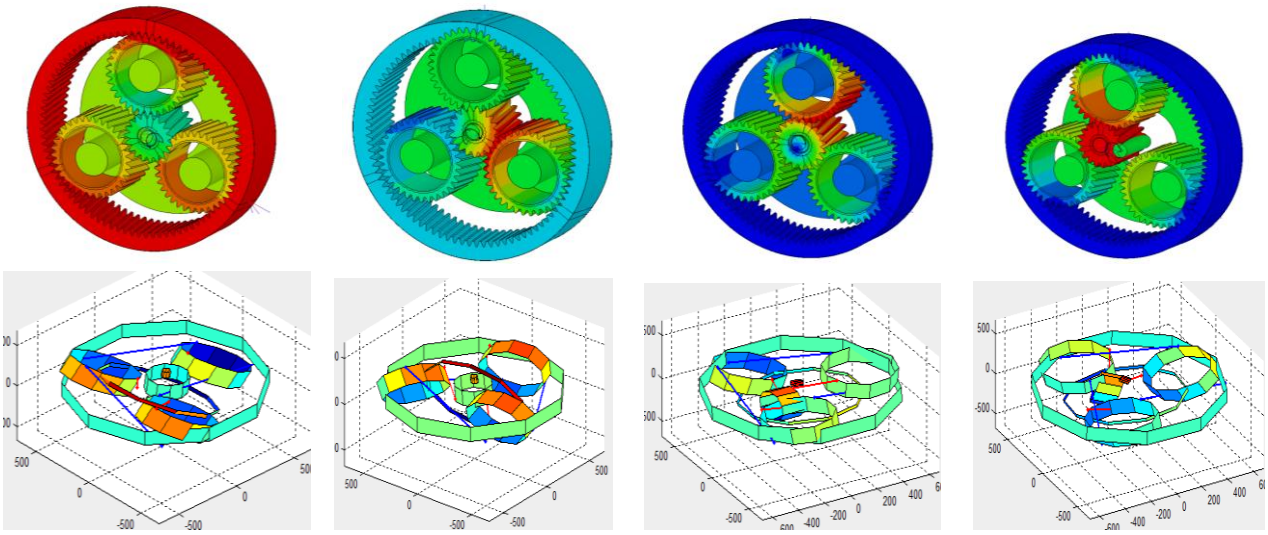

（a）76.8 Hz　（b）133.4 Hz　（c）130.9 Hz　（d）222.48 Hz

圖7. 以FEM分析之螺旋行星齒輪系之模態範例圖示(上: LS-DYNA; 下: 3D 離散):（a）平移模態76.8 Hz;（b）平移模態133.4 Hz;（c）旋轉模態130.9 Hz;（d）平移模態222.48 Hz

5.3 動態變形與動態嚙合力

5.3.1 固定轉速運轉

本研究之單級增速齒輪箱以連結行星架的輸入軸為以輸入動力，再由行星齒輪嚙合齒輪對將動力由連結太陽齒輪之輸出軸，輸入軸(行星架)為固定轉速=20rpm，輸入扭矩=3×10^5 Nm，系統阻尼比0.005，靜止初始條件，運轉條件為瞬間啟動模式，但(16)式中之$\ddot{\mathbf{X}}_R$不考慮，並設定輸出軸迴轉自由度為固定，圖9所示為在0.4秒等速間所獲得之動態變形，而圖10a、b為太陽齒輪與3個行星齒輪和環齒輪與3個行星齒輪嚙合時，外/內齒輪對之動態嚙合力隨嚙合角度之變化情形。圖10c為行星齒輪與支撐銷間動態力大小，此為軸承所承受的動態負荷，本研究已獲得行星式螺旋齒輪箱之暫態與穩態響應分析方法特性與結果。

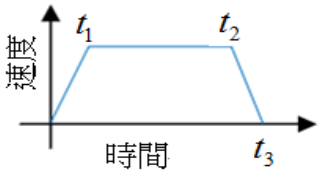

圖8. 速度-時間梯形圖

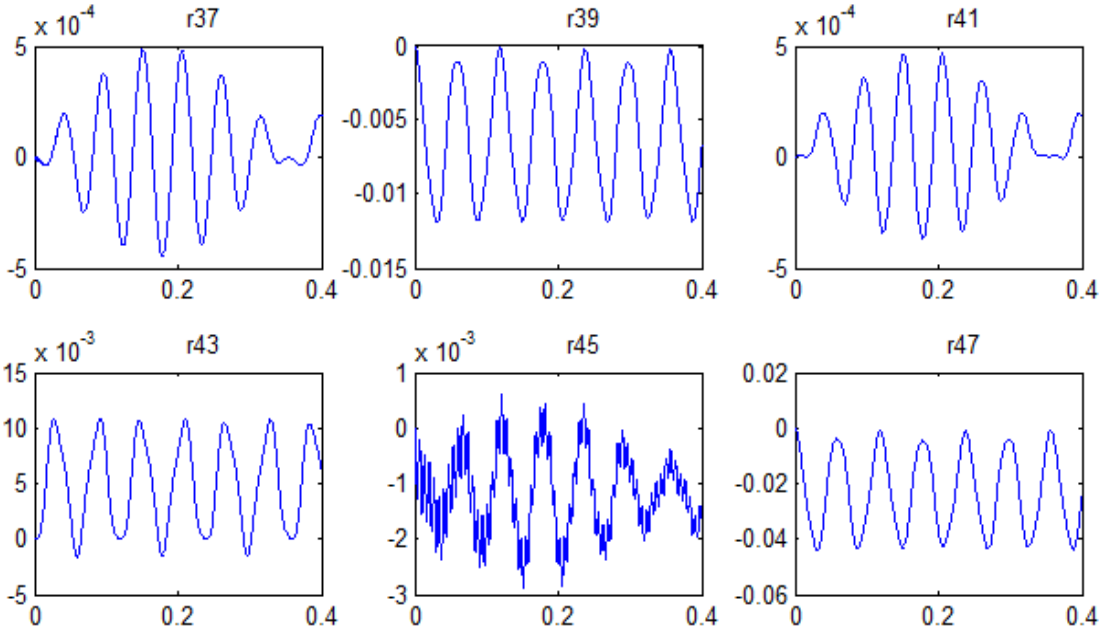

圖9. 單級行星齒輪系統之行星齒輪的6自由度動態變形響應結果

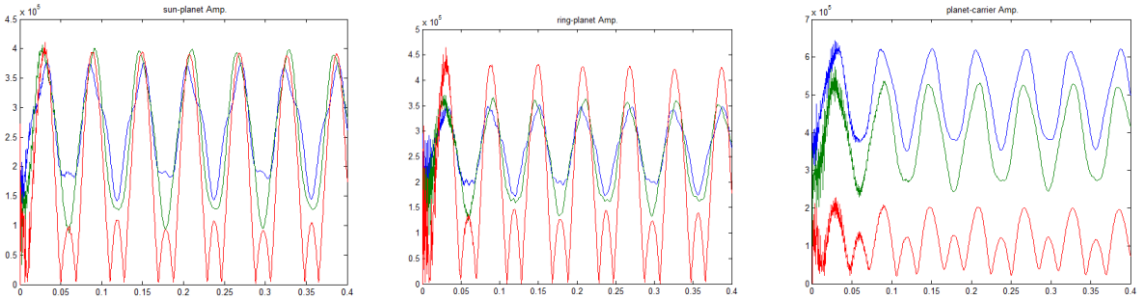

(a) 太陽齒輪與行星齒輪　(b)太陽齒輪與行星齒輪　(c)行星齒輪與支撐銷軸承

圖10. 單級行星齒輪系統之動態力

5.3.2 變動轉速運轉

前小節運轉條件可視為瞬間起動模式，以下應用離散模式分析行星齒輪系包括起動、停機等變動轉速運轉的動態特性，即(16)式中之$\ddot{\mathbf{X}}_R$不為零，設定總運轉期間為0.4秒，從靜止條件開始進入如圖8等加速時間t_1=0.04秒並加速到20rpm，之後0.32秒期間維持20rpm等速運

轉、最後(t_3-t_2)=0.04秒速期間等減速到停止，並設定為全負載操作，圖11所示為行星齒輪系在0.4秒期間之動態變形特性，顯示與圖9結果比較，剛體運動影響小僅約為2%，圖12為行星齒輪與各齒輪或行星銷之間的動態作用力。本研究已獲得行星式螺旋齒輪箱在變動負載與變動轉速之暫態與穩態響應分析方法特性與結果。

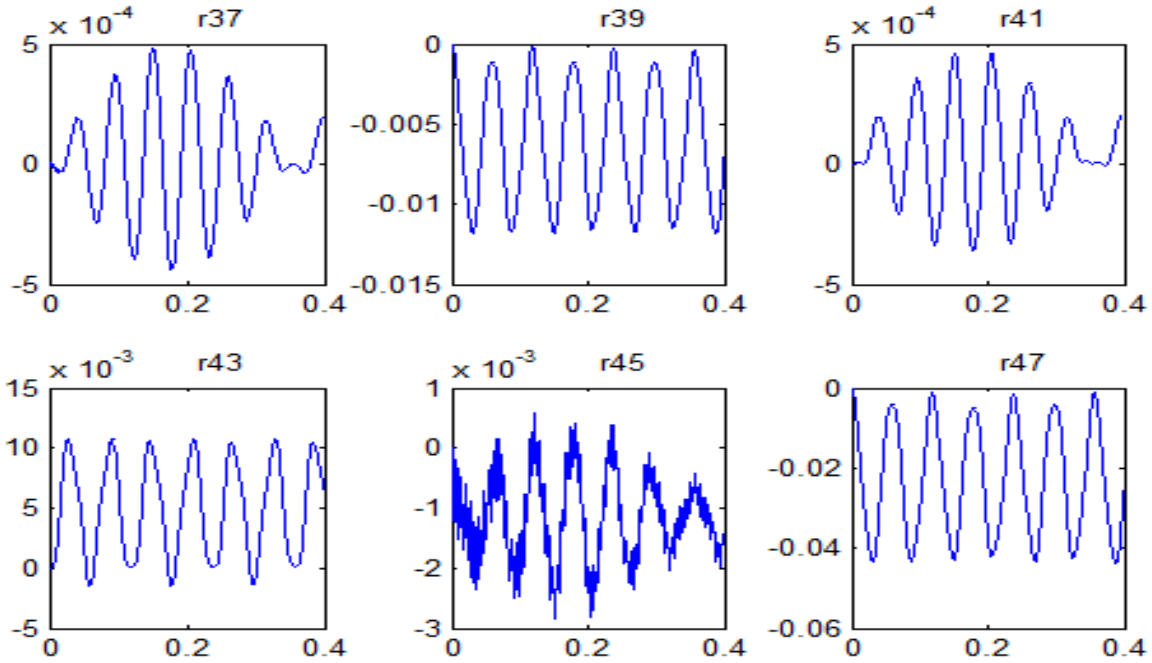

圖11. 單級行星齒輪系統之行星齒輪的6個自由度動態變形響應結果

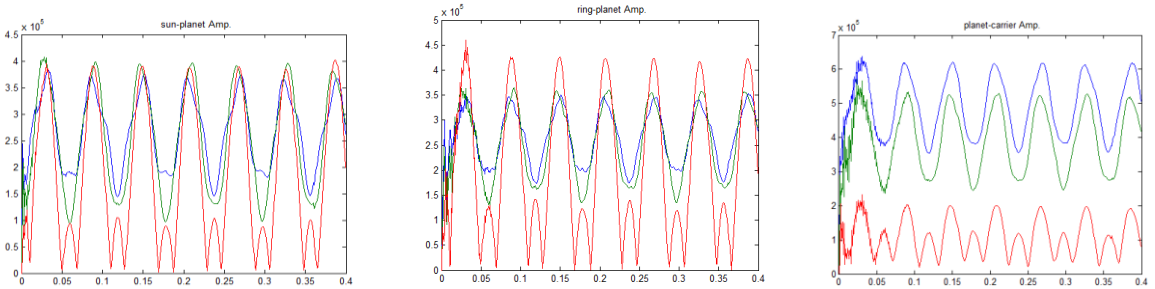

(a) 太陽齒輪與行星齒輪　(b)太陽齒輪與行星齒輪　(c)行星齒輪與支撐銷軸承

圖12. 單級行星齒輪系統之動態力

6. 結論

掌握增速齒輪箱動態特性為提升風力機組可靠度關鍵的課題，本計畫已完成兩種分析模式之行星齒輪系統動態特性探討包括非線性時變等效離散模式與LS-DYNA有限元素分析模式。在離散模式方面，完成非線性時變內/外螺旋齒輪對之等效嚙合剛度計算，可考慮齒輪對相位關係以及組裝與幾何關係，也推導出可包含剛體運動效應之影響單級螺旋行星齒輪系離散運動方程式，包括軸承、輸出入軸、齒輪箱體剛性以及變動負載等，並可以依據風場與操作資料以獲得輸出入軸的變動負載以計算行星齒輪系統的動態特性，獲得動態齒輪應力與動態軸承負載計算，並且以平均嚙合剛度計算自然頻率與模態。另外也應用有限元素的動態分析進行初步驗證。本計畫所完成理論分析模式可以考慮風場條件與扭矩變動之關係，探討各種變動負載下行星式螺旋齒輪箱之暫態與穩態響應特性。並已獲得大型風力機用單階行星式螺旋齒輪箱機組包括起動、停機等各種負載運轉條件動態特性的分析技術與數值成果，本研究若持續推展，必定可以完成國內大型風力機用增速行星齒輪箱以及如汽車傳動等各種高階齒輪傳動系統的設計分析技術建立。

參考文獻

1. T. J. Chang, Y.T. Wu, H. Y. Hsu, C. R. Chu, C. M. Liao, 2003, “Assessment of Wind Characteristic and Wind Turbine Characteristic in Taiwan,” *Renewable Energy*, Vol.28, pp.851-871
2. Industrial Wind Action Home page Homepage: http://www.windaction.org
3. Maag Homepage, http://www.maag-gear.com
4. General Electric Homepage, http://www.genergy.com/businesses/ge_wind_energy/en/index.htm.
5. Y. C. Chen and C. B. Tsay, 2002, “Stress analysis of a helical gear set with localized bearing contact,” *Finite Elements in Analysis and Design*, Vol.38, pp. 707-723.
6. F. Cunliffe, J. D. Smith, and D. B. Welbourn, 1974, “Dynamic Tooth Loads in Epicyclic Gears,” *ASME Journal of Engineering for Industry,* pp. 578-584.
7. R. August and R. Kasuba, 1986, “Torsional Vibrations and Dynamic Loads in a Basic Planetary Gear System,” *ASME Journal of Vibration, Acoustics, Stress, and Reliability in Design,* Vol. 108, pp. 348-352.
8. A. Kahraman, 1994, “Planetary Gear Train Dynamics,” *ASME Journal of Mechanical Design,* Vol. 116, pp.713-720.
9. P. Velex and L. Flamand, 1996, “Dynamic response of planetary gear trains to mesh parametric excitations,” *ASME Journal of Mechanical Design,* Vol. 118, pp.7-14.
10. T. Sun and H.Y. Hu “Nonlinear Dynamics of a Planetary Gear System with Multiple Clearances,” *Mechanism and Machine Theory,* Vol. 38, pp. 1371-1390.
11. C. Yuksel and A. Kahraman, 2004, “Dynamic Tooth Loads of Planetary Gear Sets Having Tooth Profile wear,” *Mechanism and Machine Theory,* Vol. 39, pp. 695-715.
12. R. B. Parker, 2000, “A Physical Explanation for the Effectiveness of Planet Phasing to Suppress Planetary Gear Vibration, ” *Journal of Sound and Vibration,* Vol. 236, pp. 561-573.
13. H. Ligata, A. Kahraman, and A. Singh, 2008, “An Experimental Study of the Influence of Manufacturing Errors on the Planetary Gear Stresses and Planet Load Sharing,” ASME Journal of Mechanical Design 130(4), pp. 041701.1-041701.
14. D. R. Kiracote and R. B. Parker, 2007, “Structured Vibration Modes of General compound Planetary Gear Systems, ” *ASME Journal of Vibration and Acoustics,* Vol. 129, pp.1-16.
15. M. Inalpolat and A. Kahraman, 2008, Dynamic modelling of planetary gears of automatic transmissions, *Proceedings of the Institution of Mechanical Engineering, Part K: Journal of Multi-body Dynamics,* Vol. 222(3), pp.229-242.
16. 陳建羽，2008，正/螺旋行星齒輪系統動態特性之研究，私立中華大學機械系碩士論文，新竹市。

附錄

本計畫研究計畫成果已發表三篇研討會論文:

1. 廖景輝、黃國饒*、曾瑞堂，2011，“大型風力機用多階齒輪傳動系統之特性分析”，2010臺灣風能學術研討會，澎湖。
2. 邱晨熙、傅康晏、黃國饒*，2011，“曲齒聯軸器之電腦輔助設計與實體建模”，第14屆全國機構與機器設計學術研討會論文集，桃園。
3. K. J. Huang*, C. C. Chen, and J. Y. Chen, 2007, “A finite element investigation to modal and dynamic behaviors of planetary gearings concerning the effect of bearing and carrier stiffness,” DETC *2011 12th International Power Transmission and Gearing Conference,* Las Vegas, USA. (EI)
4. 本計畫研發學術水準與工程應用皆與國際研究相當，並預計於101年4月投稿於國際期刊ASME Journal of Mechanical Design.

國科會補助專題研究計畫項下出席國際學術會議心得報告

日期：100 年 9 月 15 日

計畫編號	NSC － 2221 － E － 216 － 003		
計畫名稱	應用非線性時變模式之大型風力機用增速行星齒輪箱承受變動負載之動態響應分析		
出國人員姓名	黃國饒	服務機構及職稱	中華大學機械系教授
會議時間	100 年 8 月 28 日至 100 年 9 月 1 日	會議地點	美國 Washington DC
會議名稱	（中文） （英文） 2011 ASME International Design Engineering Technical Conferences (DETC 2011)		
發表論文題目	（中文） （英文） A finite element investigation to modal and dynamic behaviors of planetary gearings concerning the effect of bearing and carrier stiffnesses		

一、參加會議經過

- 8/26 上午(台灣時間) 至台灣桃園機場搭 UA-852 飛往日本東京，轉搭 UA-804 飛往美國 Dulles International airport,
- 8/26, 22:00 左右 (美國時間) 到達 **Washington DC**，入住 Capitol Skyline hotel。
- 8/27, 參觀 Smithsonian Institution 所屬之 Air and Space Museum.
- 8/28- 8/31 (美國時間) 全程參加 IDETC 2011，共聆聽了約 50 篇之論文發表，並提問討論。
- 8/28 (美國時間) 報到並參加 W5 之 Workshop Precision Structronic and Mechatronic Devices with Smart Materials。
- 8/29, 18:00 晚間(美國時間) 參與歡迎自助餐會，與各地相關研究學者討論交流。
- 8/30, 12:00 (美國時間) 參加 PTG 之午宴，並與多位美日齒輪研究學者進行討論交流。
- 8/31, 13:40-15:10 (美國時間) 進行本次發表之論文宣讀約 22 分鐘、回答相關提問。
- 9/1 早上 (美國時間) 至 Dulles International airport 機場搭 UA-803，於東京轉 UA-853 機返台。
- 9/2, 20:00 晚上(台灣時間) 抵台灣桃園機場。

二、與會心得

此次是本人歷次參加於國外舉辦之大型國際學術研討會，由於 PTG division 主辦單位用心與個人事先充分準備，感到是收獲最為豐碩一次，瞭解相關國際視野與個人研究信心。本屆 IDETC 2011 之 11th International Power Transmission and Gearing Conference (PTG11)中，共有齒輪與傳動系統之研究論文共約 70 篇論文，主要包含 Design and Analysis, Dynamics and Noise, Strength and Durability 之領域論文為最多。本人此次發表之論文為提出關於以 Ls-dyna 進行行星齒輪系統之模

態與動態分析方法，將可以應用於廣泛行星齒輪系統之動態研究與設計應用，口頭報告結束後並與現場提問者交流討論。此外全程參與研討會各分組之論文發表，共聆聽了約 50 篇之論文發表，包括 Design and Analysis, Dynamics and Noise, Strength and Durability, manufacturing, Plastic Gears, Wind Turbine Gears 相關研究為主，並與論文發表者進行討論，討論到關於如螺旋齒輪對應力分析、塑膠齒輪材料特性，FE 之接觸問題、齒輪潤滑實驗、非線性動態模式、行星齒輪系統之非線性動態模式與響應等課題。另則邀請 The Ohio State University Prof. Khrarman 就齒輪研究發展與方向發表演講，他就齒輪材料、設計、動態、疲勞、潤滑提出看法。會議中場休息以及用餐時間，則多與各國產學與會者交談，包括 Ohio State U.之 Gear Lab, 川崎重工之 T. Matsuoka, U. of Cincinnati 之 T. C. Lim, 鳥取大學之，GM Powertrain 之 H. Xu PhD.，Tennessee Tech U. 之 Prof. K.L. Ting，Moog Inc. 之 A. Wang 等 進行廣泛交流。本人此次參加 IDETC 2011 國際研討會，雖然會議時間只有四天(28-31 日)，收穫感觸皆多。

三、考察參觀活動(無是項活動者略)

無

四、建議

個人認為，雖然齒輪在許多應用領域已經可以完全以電力馬達模式移予以取代或省略，但隨著產業發展未來新開發出來需求應用恐怕只會更多，包括汽車、航空太空、能源與環保、精密機械、生醫等產業 ，在未來齒輪系統各領域之發展仍有無限發展的空間，包括更高的性能:如更高轉速，更大傳動體積能量比，更精密的傳動，更長的壽命以及更可靠的運轉;更低成本。應用各種技術方法，包括新材料、新齒形、新潤滑、新加工技術、新應用以及其他等零組件與新系統整體技術之設計與製造技術整合。隨著當今台灣著重環境保護與永續能源，或高附加價值產業之發展，本校位於新竹應有所投注，尤其關於大型風力發電系統用齒輪系統之發展，包括更大發電容量、振動噪音防治、可靠度、系統整合之研究，建議國內在考慮彰顯特色與永續經營時，此領域是特別值得注意投入的。另外，也建議對於大型重點之國際研討會之補助應多予以鼓勵。

五、攜回資料名稱及內容

會議手冊、論文集光碟片

六、其他

此次會議中 IDETC11-PTG11 特別有安排一個很特別的 Pipeline 的 Session，其目的在建立產業界與學界之連結，包括產業界之 FIAT(汽車)，Boeing(航空)、Wind turbine(風力發電)、Gleason Works(齒輪設計加工設備)等巨擘之技術研發最高層(皆為副總裁等級)進行演講、這些菁英領袖皆對其所屬之產業領域，未來對於傳動系統需求與已提出，包括新材料、新齒形設計、新潤滑方法、新加工技術以及其他等零組件與新系統整體技術之技術整合，內容極為精闢充實，從這謝內容可以看到未來頂尖產業於齒輪與傳動領域之發展方向，讓人耳目一新且深受動處。在參加過許多次國內外研討會，這種形式之產學聯結與溝通是很值得學習的。

kjhuang

寄件者: <Toolboxhelp@asme.org>
收件者: <kjhuang@chu.edu.tw>
副本: <timothy.l.krantz@nasa.gov>
傳送日期: 2011年5月20日 下午 10:12
主旨: DETC2011-47136 - Draft Paper Accepted

*** This is an auto-generated e-mail. There is no need to respond. ***

Congratulations Kuo Jao Huang!

The draft you have submitted to IDETC/CIE 2011 has been accepted. The final version will be eligible for publication in the conference proceedings, provided all required materials and forms are submitted by the stated deadline.

You and your co-authors will receive a separate email message with instructions for completing the Electronic Copyright agreement. You will not be able to submit your final paper until all authors have signed this form.

Your paper information is as follows:

Paper Number: DETC2011-47136
Paper Title: A finite element investigation to modal and dynamic behaviors of planetary gearings concerning the effect of bearing and carrier stiffnesses

Please incorporate the reviewer comments and my comments into your final version. The detailed comments of the reviewers are available at the http://www.asmeconferences.org/idetc2011 web site. Please log in as Returning Author to see these comments.

--- My Comments ---

The paper has been accepted for content. However, it is mandatory to revise the paper to the final ASME format (2 columns, single spaced, particular headings) per the ASME guidelines

see
https://www.asmeconferences.org/IDETC2011/FinalPaperReq.cfm

--- End Comments ---

When you have completed your final version and all authors have signed the Electronic Copyright Agreement, please login to your IDETC/CIE 2011 author account and submit it online. You will receive on-screen confirmation of your submission, as well as an e-mail confirmation.

Congratulations again and thank you for your interest and participation in IDETC/CIE 2011.

_____ Timothy Krantz
Review Coordinator
http://www.asmeconferences.org/idetc2011

*** This is an auto-generated e-mail. There is no need to respond.***

Proceedings of the ASME 2011 International Design Engineering Technical Conferences & Computers and Information in Engineering Conference
IDETC/CIE 2011
August 29-31, 2011, Washington, DC, USA

DETC2011-47136

A FINITE ELEMENT INVESTIGATION TO MODAL AND DYNAMIC BEHAVIORS OF PLANETARY GEARINGS CONCERNING THE EFFECT OF BEARING AND CARRIER STIFFNESSES

Kuo Jao Huang
Department of Mechanical Engineering
Chung Hua University,
No. 707, Sec. 2, Wu Fu Rd, Hsin Chu, Taiwan

Shou Ren Zhang
Department of Mechanical Engineering
Chung Hua University,
No. 707, Sec. 2, Wu Fu Rd, Hsin Chu, Taiwan

ABSTRACT

A finite element (FE) method is used to analyze modal and dynamic behavior of planetary gear systems (PGSs) focusing on the effect of bearing and carrier stiffness. Using derived tooth profile equations, elements for gear can be parametrically created. Then, the 2D/3D FE models of a planetary gear system (PGS) are constructed. Accordingly, structural natural frequencies and modal shapes are calculated after adequately assigning the material, boundary conditions, and tooth contact of gear pairs. An index, namely dimensionless slope, is defined to reflect the modal property due to the bearing stiffness change. Influence of carrier material and gear bearing stiffnesses on modal behavior is investigated. Several results of the PGS modal characteristics affected by the material and bearing stiffness are also obtained. Besides, the dynamic responses of the PGSs are analyzed under the carrier rotation. Finally, dynamic fillet stress and loading inequality among gear pairs due to planet bearing stiffness variation are analyzed. The FE approach presented can conveniently demonstrate modal and dynamic behaviors of PGSs.

INTRODUCTION

Because of the excellent feature of high power density, high reliability, and low noise and vibration, planetary gear transmission has been well applied in the wide field of industries including vehicles, aircrafts, wind turbines, and robots etc. To date, endeavors for its performance improvement especially in the dynamic aspect are still continued. Of some simplicity and efficiency the equivalent discrete mass-spring method is normally used in the gear dynamics. Therefore, two works to obtain the equivalent stiffness of spur gear pair are exemplified [1, 2]. Hedlund [3] calculated the tooth deflection of a helical gear pair by combining the Hertzian contact analysis and tooth foundation flexibility. Kahraman [4] presented a three dimensional (3D) discrete model to investigate the helical PGS dynamics in which modal shapes and dynamic forces resulting from static transmission errors were investigated. Furthermore, the author also categorized planet phasing conditions and emphasized that the categorization was primarily for compatibility but might cause misleading in the 3D model for gears. In addition, Sadda and Velex [5] considered torsional, flexural, and axial generalized displacements of components including finite element procedure. In their study, a complex planetary gearing was simplified to a discrete twelve degrees-of-freedom system. Furthering their previous works, Velex and Flamand [6] indicated the stiffness of meshing gear pairs has more significant effect on planetary dynamic behavior than other components. In recent years, plentiful studies in planetary gear dynamics were presented [7-9]. The authors analyzed the modal behaviors of PGSs including three- and four-planets of equally spacing and diametrical symmetry with planet meshing phase difference (MPD) or not using linear or nonlinear models. For example, Lin and Parker [7] calculated natural frequencies of PGSs in which the nonlinearity due to meshing stiffness discontinuity of gear pairs was discussed. In the study [10], using the modal analyses and mesh phasing properties, design rules are analytically derived to suppress specific harmonics of plant modal response of a PGS. Recently, using a nonlinear discrete vibration model, Al-shyyab and Kahraman [11] investigated influences of time-varying meshing stiffness, contact ratio, and backlash on the dynamic responses of single-stage PGSs. Extending this to multistage gears, Inalpolat and Kahraman [12] presented a generalized dynamic model applied to several types of complex PGSs. The influence of coupling stiffnesses and kinematic configurations on the natural modes and dynamic responses of a three-stage automotive

transmission application was demonstrated. In addition, Farshidianfar et al. [13] investigated the nonlinear vibration of single-stage gearing using several analyzing methods. The authors indicated that all the methods are effective in calculating the dynamic spectrum but only two of them are adequate to identifying the gearing modal property.

The equivalent discrete models in gear dynamics may significantly simplify modeling complexity and numerical computation. However, using a discrete model in gear dynamics is cumbersome since abundant knowledge and technique must be prepared such as meshing stiffness, backlash, and error models etc. Alternatively, the continuum approaches using the FE or the stiffness methods were attempted [14-16]. Nevertheless, on account of strict element requirement of quantity and quality in dealing with the tooth contact problem, complex PGS dynamics entirely using the FE is still limited. Therefore, the FE approach combining a semi-analytically integral process was presented to help the reduction of elements in dealing with tooth contact problem [17]. Basing on that, Parker et al. [18] performed a PGS dynamic investigation focusing on the modal and harmonic behavior. Besides, a few of special-purpose packages for gearing dynamics were developed but limitation including modeling constraints, gearing types, or cost remains. To the authors' best understanding, it is still a hard task to fulfill detail modal and dynamic properties in kinds of PGSs using an FE method. Therefore, in this study, an FE approach using a general purpose package to the modal and dynamic analyses of PGSs is undertaken. Moreover, Influences of bearing and material stiffnesses on their modal characteristics will be discussed accounting for floating or rigid design, the bearing stiffness is assigned from a very soft value to a rather rigid one basing on a reference stiffness of 10^8 N/m. Finally, the dynamic responses of the PGSs are analyzed. Non-uniformity of dynamic fillet stresses among gear pairs due to bearing stiffness variation is investigated.

CONSTRAINTS AND FE MODELS

Assembly Constraints and Phase Difference

The following constraints are required on the PGS construction. A planetary gearing can be assembled if the angular position of planet gears satisfies

$$\frac{\left(z^s + z^r\right)\psi_c^k}{2\pi} \in \text{Int} \tag{1}$$

where "Int" denotes integer, ψ_c^k is the distributing angle of kth planet gear positioning around the sun gear as illustrated in Fig. 1, and z^s and z^r are the numbers of teeth for the sun and ring gears, respectively. To an equally spacing PGS, the sum of tooth numbers of planet and ring gears can be integrally divided by quantity number of planet gears, i.e.,

$$\frac{z^s + z^r}{n} \in \text{Int} \tag{2}$$

where n is the number of planet gears. More specifically, to fulfill an equally spacing gearing of non MPD it requires

$$z^s / n \in \text{Int} \quad \text{and} \quad z^r / n \in \text{Int} \tag{3}$$

Beside, the MPD angle $\Delta\theta_p^k$ between the kth and 1st sun-planet (s-p) or ring-planet (r-p) pairs can be calculated using Eq. (4) [19].

$$\Delta\theta_p^k = [z^s - \text{Int}\left(z^s / \left(2\pi/\psi_c^k\right)\right) \times \left(2\pi/\psi_c^k\right)] / \left(2\pi/\psi_c^k\right) \times \left(2\pi/z^p\right) \tag{4}$$

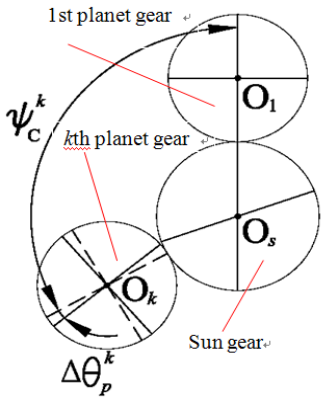

Fig. 1 The distributed angle interval ψ_c^k between the kth and 1st planet gears for calculation of MPD

FE Model

The process of tooth profile derivation and element creation for gears are entailed in a previous work [20]. Only briefing description is given. The profile equations including tooth blank and fillet are deduced basing on a rack cutter through coordinate transformation together accompanying with the equation of meshing for gears [21]. When analyzing gear dynamic responses, fine description of tooth profiles using elements is utmost essential, especially analyses to obtain the local contact stress or bending fillet stress in gears. For this reason, FE model of gears in this study are carefully constituted with mapped elements which are directly and parametrically built from the tooth profile equations. Through which, element distribution and density of teeth and blank of gears can be conveniently regulated so as the precise geometry of tooth profile is attainable.

A detailed illustration of the elements around the contact region of a meshing tooth pair is given in Fig. 2(a). The penalty method accompanying a slave search algorithm is used in dealing with the contact problem by placing normal interface springs between all penetrating nodes and the contact surfaces of tooth pairs [22]. Besides, in order to ensure the mating gears, being of single tooth pair in contact with a single mating surface pair, to facilitate this continuum modal analysis of PGSs, a skilled step is taken as shown in Fig. 2(b) at which the teeth participating in the contact are separated from their parent gears and to be individual parts [22]. In this study, only single

tooth pair in contact is considered. In case of double tooth pairs in contact concerned, stiffness of a gear pair can be assigned being roughly doubled but no further discussion here. However, it is emphasized again this separating step is required only in dealing with modal analyses. Afterwards, the shafts, carrier, and other components are also attached, each bearing, not two perpendicular springs, is simulated using three equally spacing springs to reduce directional stiffness unevenness. Finally, the completed 2D/3D FE models are shown in Fig. 2 but only the 2D element model will be continued in the following modal and dynamic analyses.

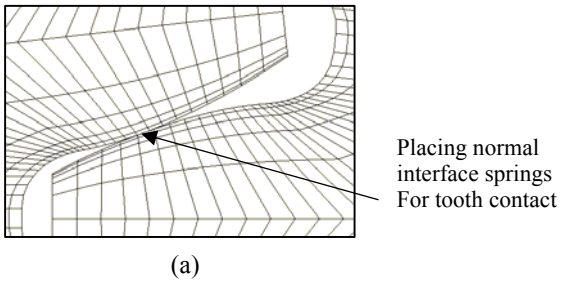

(a)

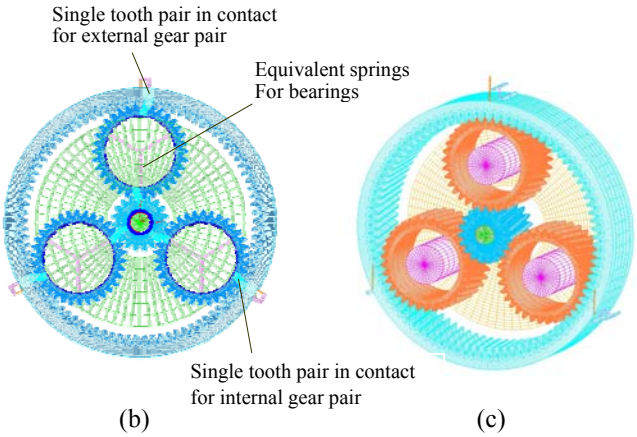

(b) (c)

Fig. 2 FE models: (a) detail showing around contact region; (b) 2D model; (c) 3D model

Categorization of Modal Shapes

According to the previous works basing on the discrete models [4, 7], modal shapes of PGSs are categorized into the three kinds of modes of translation, rotation, and planet, respectively as illustrated in Fig. 3. For identification, Ti, Ri, and Pi denote the *i*th modes of translation, rotation, and planet modes, respectively. The repetition of translation modes is two. The planet modes appear only when the number of planets is larger than three. A PGS having *n* planet gears (n>3) always exhibits three planet vibration modes of repetition n-3. Therefore, in the case of four-planet system as shown in Fig 3, its planet natural mode has repetition one.

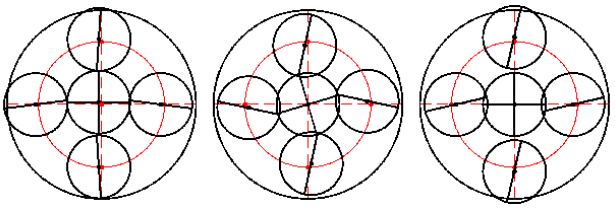

(a) Ti (b) Ri (c) Pi

Fig. 3 Three categories of modal shapes for a PGS with four planets: (a) Translation mode Ti; (b) Rotation mode Ri; (c) Planet mode Pi

A MODAL ANALYSIS OF PGS

A three-planet PGS (19-34-89) with MPD is analyzed whose gear data are given as: module m_n=16mm, pressure angle $\alpha_n = 20°$, teeth numbers of gears z^s=19, z^p=34, and z^r=89. The FE models have been shown in Fig. 2. Young's modulus of all components $E = 0.206\times10^6$ MPa and the bearing stiffnesses $k_B = 10^8$ N/m. Then, using the 2D FE model in Fig. 2(b), 13 structural translation modes (Ti) and 3 structural rotation modes (Ri) are calculated out and depicted in Table 1. Noticeably, frequencies to the translation modes cannot doubly appear even their value shows close such as two frequencies pairs (47.4, 48.5) and (82.9, 97.4) for examples. There are no double translation modes for the kind of equally spacing PGS with MPD. Perfect repetition in translation modes cannot occur is arisen from the slight deviation of meshing stiffness among gear pairs. The result is a little different from the gear dynamic studies of discrete model since in which the average of meshing stiffness are generally assumed. Thus, the slight stiffness deviation is not concerned. No planet modes exist for the three-planet PGS. To visualize the resulted modal shapes, two vibration modes of T5 and R4 are shown in Fig. 4.

Additionally, there are three additional modal frequencies of CR1= 899.7 Hz and CT1= CT2=2329.0 Hz resulted. Those modes are respectively corresponding to rotational and translational deformations of the carrier. Besides, it exhibits that the translational one has a repetition number of two. Actually, these modes are not structural vibration modes. Nearly, they only associate with the componential formation of carrier. Consequently, they will not be furthered on discussing the influence of bearing stiffness on structural modal frequencies but on the material stiffness effect of carrier afterwards.

STIFFNESSES AND PGS MODAL BEHAVIOR

Change of Systematical Bearing Stiffness

The gearing (19-34-89) data has been given above. Also, bearing stiffness $k_B = 10^8$ N/m is assigned as a reference value. Basing on that, the influence of difference systematical bearing stiffnesses on gearing modal behavior is discussed. Systematical means all bearing stiffnesses supporting the components in a PGS are wholly changed. Because the support

method in PGSs may be from completely floating to very rigid, the value of bearing stiffnesses is assigned from a softer one of 10^7 N/m, i.e. 0.1 to 100 times of the reference stiffness of 10^8 N/m. Then, the calculated structural natural frequencies of the gearing corresponding to various stiffness assignments are shown in Fig. 5(a). The result shows all structural frequencies are increased when increase systematical bearing stiffnesses. Moreover, by selecting the curve of R2 as a dividing border, the 16 natural frequencies can be categorized into two groups: one is the lower frequency group (shown by dashed curves) including 10 lower frequency modes of R1 and T1 to T9, and the other one is the higher frequency group (shown by continuous curves) including 6 higher frequency modes of R2, R3, and T10 to T13. The result in Fig. 5(a) also exhibits that the frequencies of the lower group are more significantly increased especially as the systematical stiffnesses are 10 times increased or more.

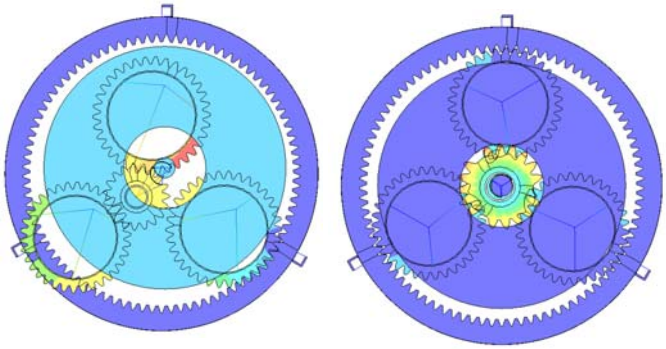

(a) (b)

Fig. 4 Two examples of resulted modal shapes: (a) T5 (138.0 Hz); (b) R3 (2349.4 Hz)

Subsequently, an index Ω called dimensionless slope is used to further expose the change tendency and sensitivity of natural frequencies for structural vibration modes due to the bearing stiffness change which is defined. Thus,

$$\Omega_i = \frac{(\omega_i - \omega_{i-1})/\omega_{i-1}}{(k_{B,i} - k_{B,i\text{-}1})/k_{B,i\text{-}1}} \tag{5}$$

where ω_i and Ω_i denote the calculated natural frequency and dimensionless slope under the assigning bearing stiffnesses $k_{B,i}$. Accordingly, the obtained dimensionless slopes from the result in Fig. 5(a) are shown in Fig. 5(b). The figure exhibits that the dimensionless slopes belonging to the lower group (continuous curve) are always relatively large during the assigned systematical stiffnesses which is especially obvious at a smaller assignment such as 0.5 times or lower. The bigger values of Ω's are mode T1 to T4 which implies these four frequencies are increased more evidently than the others with the increase of systematic stiffnesses. In other words, the frequencies belonging to the lower group are tending to adjustable by regulating bearing stiffnesses. Besides, the Ω's of R1 and T5 to T9 are increased more significantly of the interval between 0.1 to 2.0 times. When bearings become stiffer, their effect on vibration frequencies of these modes is also more significant. As the bearing stiffnesses are assigned about 10 times to 10^9 N/m, the most of Ω's achieve maxima that implies around which the gear modal property is very sensitive to bearing stiffness change. After that, most Ω's turn to smaller except those belong to the higher frequency group. During that, the six frequencies to the higher group are less increased comparing to the higher frequency group. However, as the bearing stiffnesses are assigned larger than 4×10^9 N/m, the increase of Ω's of the higher frequency group (dashed line) also becomes significant since near which the shapes of their vibration modes essentially transform. Since the dimensionless slope can more meaningful demonstrate modal property of PGSs, only the graphical showing of Ω's is given afterwards.

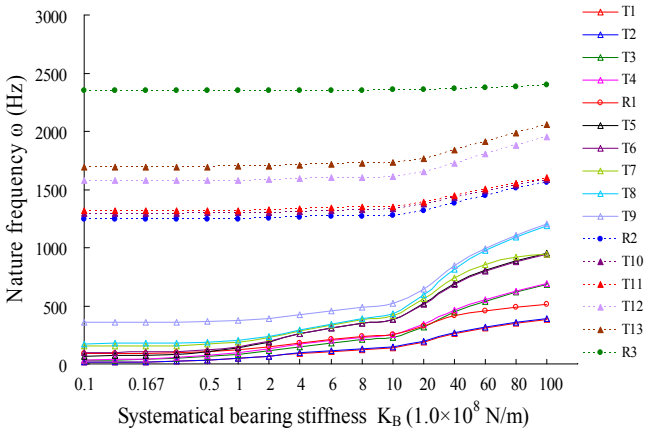

(a)

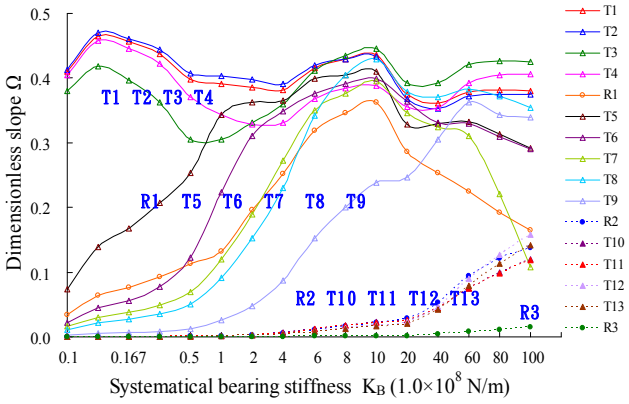

(b)

Fig. 5 Relation of structural natural frequencies ω and dimensionless slopes Ω and systematical bearing stiffness

Change of Planet Bearing Stiffness

After the above discussion by changing stiffness systematically, influence of the planet bearing stiffness is discussed. Firstly, as shown in Fig. 6, more or less, the planet bearing stiffness has an effect on all the structural modal frequencies but what modes are more affected is not same for different stiffness values. When the stiffness is increased 4 times to 4×10^8 N/m and the larger, Ω's of R1 and T5 toT9 are evidently larger than the others. Those frequencies are more affected by the change of planet bearings stiffness because they are closely relating to the rotation and translation movements of plant gears. Their maxima of Ω's are appearing around the stiffness of 10 times increase. Noticeably, the other modes which are the four lowest frequency modes of T1 toT4 and the six modes in the high frequency group are less affected by the planet bearing stiffnesses since displacements of these modes are less relating to planet bearings.

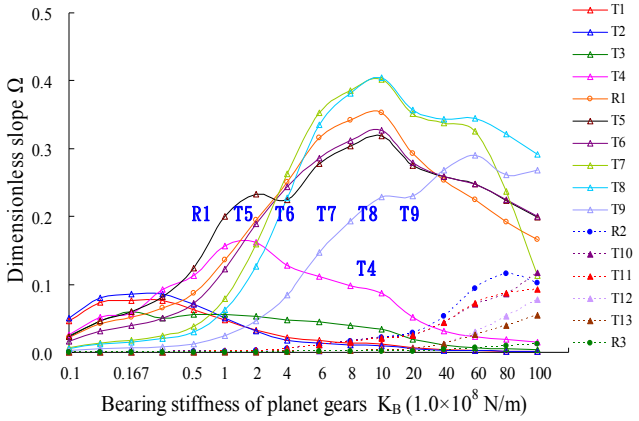

Fig. 6 Relation of dimensionless slopes Ω of structural natural frequencies and bearing stiffness of planet gears

Effect of Carrier Stiffness

Stiffness and machining accuracy of planet carrier essentially affect the gearing dynamic behavior. In this study, only the effect of carrier stiffness is analyzed by assigning various Young's modulus E. The value of 0.206×10^6 MPa is used as a reference basis value and the values between 0.206×10^6 MPa and 0.206×10^4 MPa are assigned. Figure 7 shows the calculated ω's and Ω's under various carrier moduli. The effect of Young's modulus of the carrier is almost on the modes of CR1, CT1, and CT2 only. The increasing rates of ω's and Ω's belonging to the above three vibration modes are significantly larger than the others when increase E since these three modes are closely relating to the deformation of carrier and its bearings. As the above stated, CR1, CT1, and CT2 are not structural modes but componential ones. The carrier stiffness does not evidently affect any other modal frequencies except the three modes especially for $E > 0.206\times10^6$ MPa. Even the carrier stiffness does not manifestly change the structural modal displacement characteristics of the PGS, it can be designed with adequate compliance to absorb the excitation from the design or manufacture causes.

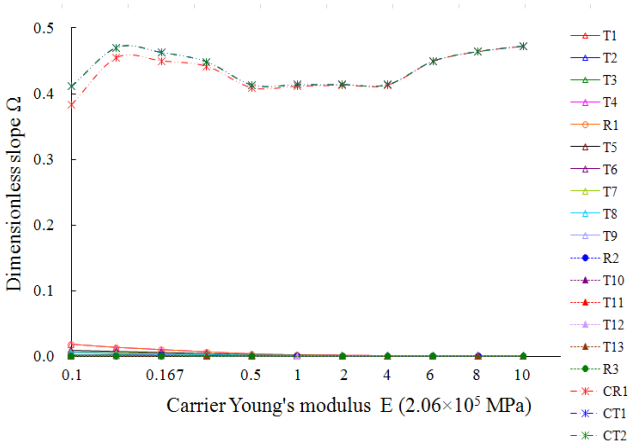

Fig. 7 Relation dimensionless slope Ω and carrier stiffness using various Young's modulus E

DYNAMIC RESPONSE OF PGS

Dynamic Fillet Stress

This section analyzes dynamic responses of the PGS. The created 2D FE model is shown in Fig. 2. At first, the rotation speed of sun gear $n^{(s)}$ =95.5 rpm. The detailed operating and gear data are depicted in Table 2. The damping effect is not incorporated. Firstly, dynamic fillet stresses of two adjacent tooth pairs for the three s-p pairs are shown in Fig. 8 at which SPi.j (PSi.j) denotes the dynamic sun (planet) gear fillet stress of the jth meshing tooth pair for the ith s-p gear pair. In this PGS analysis, i=1 to 3, j=1 and 2. For example, SP2.1 is the sun gear fillet stress of the first tooth pair for the second s-p pair. Besides the abscissas are absolute rotation angles of sun and planet gear for SPi.j and PSi.j, respectively. Similarly, RPi.j denotes the ring gear fillet stress in r-p gear pair but does not show for briefing. The dynamic fillet stresses of the two adjacent teeth in s-p pairs are shown in Fig. 8. Not only the dynamic stresses on sun gear but also those on planet gears for various s-p gear pairs are very close. To certain extent, their similarity verifies the correctness of the numerical calculation.

Subsequently, fillet stresses of SP 1.1 and SP1.2 in Fig 8(a) are more described. Three snapshots to illustrate the meshing process of tooth pairs are given in Fig. 9. At the onset of meshing process, including another leading tooth pair, the number of tooth pairs in mesh of the first s-p pair is double. When the sun gear rotation angle is between 0° and 13.8°, the dynamic fillet stress is fluctuating with the advance of tooth meshing after a rapid increasing. The dynamic fillet stress distribution at a sun rotation angle of 8° is given in Fig. 9(a). Afterwards, a leading tooth pair ends its mesh and thus the s-p pair goes into the interval of single tooth pair in contact which is the sun rotation angle between 13.8° and 22.9°. The stress

distribution at sun rotation angle 15.5° is shown in Fig. 9(b). During the interval, the observed tooth pair burdens the whole loading splitting to the first s-p gear pair. Therefore, a maximum filet stress of 198 MPa appears at the rotation angle of 15.5° since at the instant the tooth contact is around the highest point of singe tooth contact (HPSTC). Subsequently, the meshing process continues to the third step at which the second tooth pair participates. The next tooth pair starts its meshing process and thus the number of meshing tooth pairs resumes double again. The stress distribution at rotation angle 31.3° is give in Fig. 9(c). Finally, the observed tooth pair terminates its meshing cycle at the sun rotation angle of 36.5°.

Finally, the dynamic fillet stresses of SP 1.1 in the PGS at three operation speeds of 50 rpm, 95.5 rpm, and 150 rpm are calculated and shown in Fig. 10. It exhibits that a larger operation speed causes a larger dynamic response. The particular fluctuation is occurring at the speed of 150 rpm since at the speed the PGS has a meshing frequency of 39.1 Hz which very close to the sixth superharmonic frequency (38.4 Hz) belonging to mode T3 (230.5Hz).

5.2 Planet Stiffness and Loading Share Inequality

The most noticeable feature of PGS may be its load split ability, but the practical performance is closely affected by numerous designing and manufacturing factors. Next, non-uniformity of dynamic fillet stresses in the s-p and r-p gear pairs is further analyzed due to planet bearing stiffness variation. All the bearing stiffnesses in this PGS analysis are assigned to a reference value of 10^9 N/m except the bearing stiffness for the first planet gear which will be wide range adjusted between 10^7 and 10^{11} N/m. The calculated results for all the three s-p and r-p gear pairs are shown in Fig. 11 in which SPi and PSi respectively represent the dynamic stress maxima occurring in the sun and planet gears of the ith s-p pair. Similarly, RPi and PRi denote the maximum ring and planet fillet stresses for the ith r-p pair. In case that all bearing stiffnesses of planets have an identical basis value of 10^9 N/m, the maxima of planet fillet stresses for both the s-p and r-p pairs, i.e. PSi and PRi are about 198 MPa.

Finally, non-uniformity of dynamic fillet stresses due to load splitting inequality among the s-p and r-p pairs is discussed by changing the bearing stiffness of a planet. As shown in Fig. 11, when the bearing stiffness in the first planet is assigned to a lower value, the maximum fillet stresses in the first s-p and r-p pairs become less. Thus, the stresses in the other planet pairs become larger. For an example, as a softer stiffness of 10^7 N/m, the maximum planet fillet stresses are decreased to 142 MPa for the first s-p pair and to 110 MPa for the first r-p pair. However, the planet stresses for the other two are increased to 292 MPa for the second and third s-p pairs and to 228 MPa for r-p pairs. The increase of planet fillet stresses in pair 2 and 3 is caused by larger fraction of loading sharing by them. A similar changing tendency is observed in the r-p pairs. On the other hand, when the bearing stiffness of the first planet is increased to a stiff one such as 10^{11} N/m for example, the maximum stresses in the first planet is increased to 395 MPa for s-p pairs and 308 MPa for r-p pairs, owing that a larger fraction of loading is splitting to it. Naturally, stresses for the other two (pair 2 and 3) become the less values of 76 MPa for s-p pairs and 50 MPa for r-p pairs, respectively. Besides, it is worthy to point out that the stress of the first planet is (198-142)/198= 28.3% decreased only for the first s-p pair on conditioning that its bearing stiffness is two-order decreased. Also, the first planet fillet stress is (292-198)/198= 47.5% increased only if its bearing stiffness is two-order increased. The more of stiffness variation it is the more stress difference exhibits. Nevertheless, the change rate of the fillet stresses is not as significant as the planet bearing stiffness since loading sharing fractions of planets are determined by their resultant stiffnesses of all components not the bearing stiffness only.

The above result demonstrates the loading non-uniformity due to the bearing stiffness variation among planet gears. Actually, several other factors may cause loading split inequality such as unequally planet spacing, planet meshing phase, and manufacturing errors. Their investigations and the measures to improve them like floating sun gear or flexible carrier design can be furthered using the proposed method.

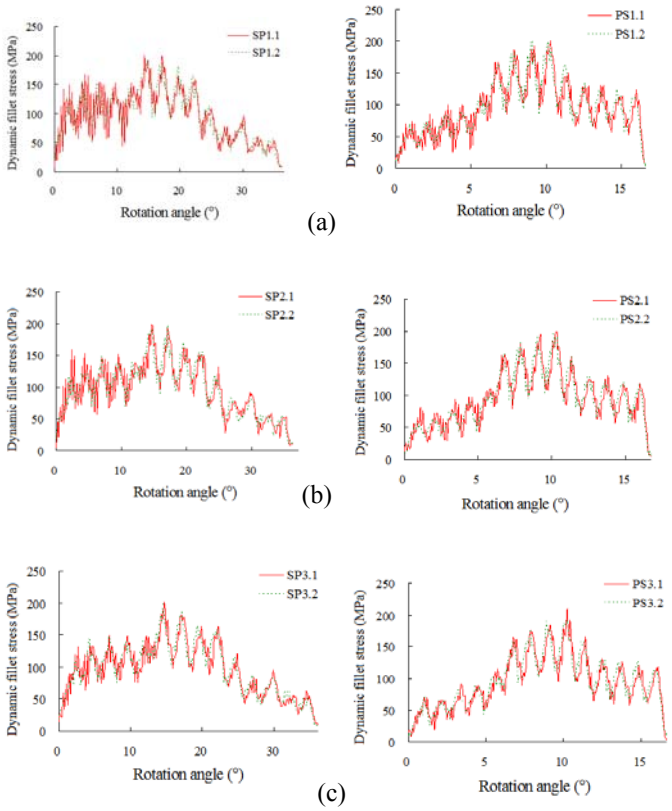

Fig. 8 Dynamic fillet stresses of two adjacent tooth pairs for three s-p gear pairs during one meshing cycle at $n^{(s)}$= 95.5 rpm: (a) 1st s-p pair; (b) 2nd s-p pair; (c) 3rd s-p pair

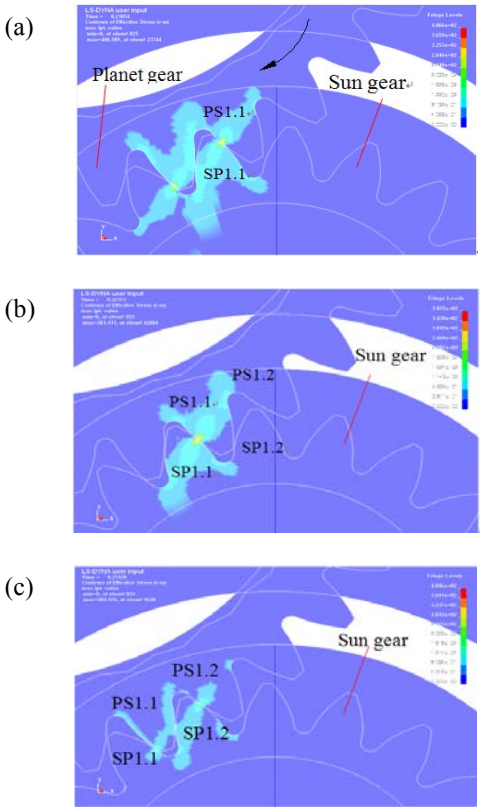

Fig. 9 The dynamic fillet stress distribution at three meshing instants for first s-p pair at sun gear rotation angle: (a) 8°; (b) 15.5°; (c) 31.3°

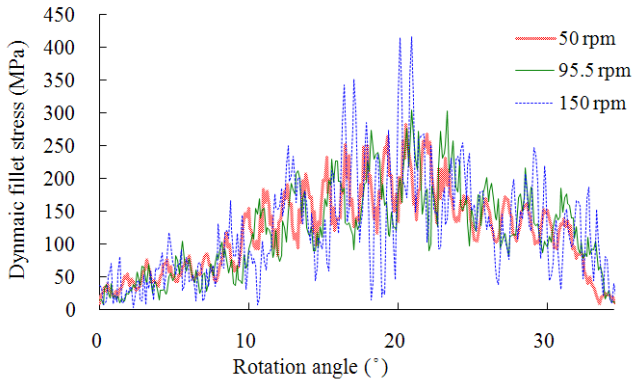

Fig. 10 The dynamic fillet stresses of SP 1.1 under three sun gear rotation speeds

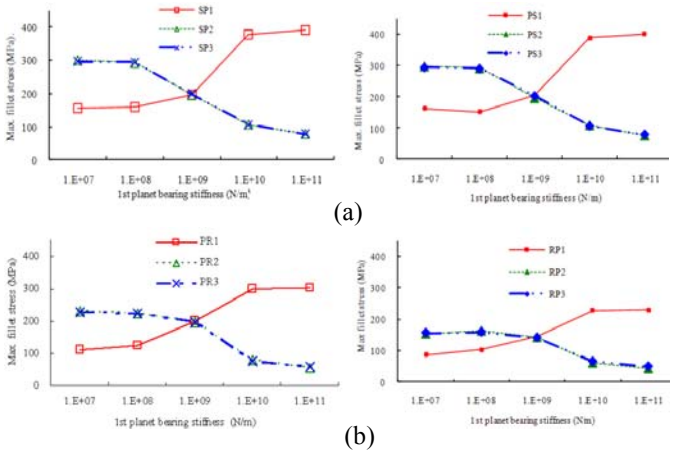

Fig. 11 Non-uniformity of maximum fillet stresses due to load sharing inequality in three gear pairs by changing one planet bearing stiffness at $n^{(s)}$= 95.5 rpm: (a) s-p pairs; (b) p-r pairs

CONCLUSIONS

This study analyzed modal and dynamic property of PGSs by an FE approach using a commercial package. The influence of systematical or componential bearing stiffness on the modal behavior and dynamic response was investigated. Also, the effect of carrier material stiffness was emphasized. Several results relating the PGS modal characteristics and stiffness were obtained. For example, the perfect repetition of translation modes is not always exactly appearing in PGSs of equal space with MPD. The structural natural frequencies of the lower group are more affected than the higher group when the bearing stiffness changes. Only the componential modes belonging to the carrier are really affected by its Young's modulus. Finally, dynamic responses of PGSs were also analyzed. Fillet stresses and their non-uniformity among s-p and r-p gear pairs were also analyzed by differing one of the planet bearing stiffnesses. The result also shows the stress change rate is not as obvious as the bearing stiffness. This FE approach in this study shows its convenience in the PGS modal and dynamic studies. Its extension to the dynamic problems of wide PGS types is also expected.

ACKNOWLEDGMENTS

The authors would like to thank the financial support from National Science Council of Taiwan, R.O.C. under the project research of NSC-99-2221-E-216-003.

REFERENCES

[1] Du, S., Randall, R. B., and Kelly, D. W., 1998, Modeling of spur gear mesh stiffness and static transmission error, *Proc. IMechE, Part C: J. Mechanical Engineering Science*, 212(4), pp. 287-297.

[2] Arafa, M. H. and Megahed, M. M., 1999, Evaluation of spur gear mesh compliance using the finite element

method, *Proc. IMechE, Part C: J. Mechanical Engineering Science*, 213(6), pp.569-579.

[3] Hedlund, A. L., 2008, A parameterized numerical model for the evaluation of gear mesh stiffness variation of a helical gear pair, *Proc. IMechE, Part C: J. Mechanical Engineering Science*, 222(7), pp.1321-1327.

[4] Kahraman, A., 1994, Planetary gear train dynamics, *ASME J. Mech. Des.*, 116(3), pp. 713-720.

[5] Saada,A. and Velex, P., 1995, An extended model for the analysis of the dynamic behavior of planetary trains, *ASME J. Mech. Des.*, 117(2), pp. 141-247.

[6] Velex, P. and Flamand, L., 1996, Dynamic response of planetary trains to mesh parametric excitations, *ASME J. Mech. Des.*, 118(7), pp. 7-14.

[7] Lin, J. and Parker, R.G., 1999, Analytical characterization of the unique properties of planetary gear free vibration, *ASME J. Vibr. Acoust.*, 121(3), pp. 316-321.

[8] Parker, R. B. ., 2000, A physical explanation for the effectiveness of planet phasing to suppress planetary gear vibration, *J. Sound Vibr*, 236(4), pp. 561-573.

[9] Parker, R. G., Agashe, V., and Vijayakar, S. M., 2000, Dynamic response of a planetary gear system using a finite element/contact mechanics model, *ASME J. Mech. Des.*, 122(3), pp. 304-310.

[10] Ambarisha,V. K., Parker, R. B., and Lin, J., 2004, Suppression of planet mode response in planetary gear dynamics through meshing phasing, *ASME J. Mech. Des.*, 128(2), pp. 133-142.

[11] Al-shyyab, A. and Kahraman, A. , 2007, A non-linear dynamic model for planetary gear sets, *Proc. IMechE, Part K:: J. Multi-body Dynamics*, 221(4), pp. 567-576.

[12] Inalpolat, M. and Kahraman, A. , 2008, Dynamic modeling of planetary gears of automatic transmissions, *Proc. IMechE, Part K: J. Multi-body Dynamics*, pp. 222(3), 229-242.

[13] Farshidianfar, A., Moeenfard, H., and Rafsanjani, A. , 2008, Frequency response calculation of nonlinear torsional vibration in gear systems, *Proc. IMechE, Part K: J. Multi-body Dynamics*, 222(1), pp. 49-60

[14] Yuksel, C. and Kahraman, A. , 2004, Dynamic tooth loads of planetary gear sets having tooth profile wear, *Mech. Mach. Theory*, 39(7), pp. 695-715.

[15] Li, C. H., Chiou, H. S., Hung, C., Chang, Y. Y., and Yen, C. C. ., 2002, Integration of finite element analysis and optimum design on gear systems, *Finite Elem. Anal. Des*, 38(3), pp. 179-192.

[16] Huang, K. J., Chen, C. C., and Chen, J. Y., 2008, Time varying approaches to dynamic Analysis of a planetary gear system using a discrete and a continuum models, *2007 Proceedings of the ASME International Design Engineering Technical Conferences and Computers and Information in Engineering Conference, DETC2007*, 7, 451-458.

[17] Vijayakar, S., 1991, A combined surface integral and finite element solution for a three-dimensional contact problem, *Int. J. Numer. Methods Eng.*, 31, pp. 525–545.

[18] Parker, R. G., Agashe V., and Vijayakar S. M., 2000, Dynamic response of a planetary gear system using a finite element/contact mechanics model, *ASME J. Mech. Des.*, 122(3), pp. 304-310.

[19] Chen, J. L. and Tseng, C. H., 2001, Assembly considerations for planet gear sets in planetary gear trains, J. Chin. Soc. Mech. Eng. Trans. Chin. Inst. Eng. Ser C, 22(3), pp. 235-239.

[20] Huang, K. J. and Su, H. W., 2010, Approaches to parametric element constructions and dynamic analyses of spur/helical gears including modifications and undercutting, *Finite Elem. Anal. Des.*, 224(2), pp. 203-210.

[21] Litvin, F. L., 2004, *Gear Geometry and Applied Theory, Cambridge*, New York, Chap 6.

[22] Hallquist, J. O., 1998, in: *LS-DYNA Theoretic Manual*, LSTC Ltd.

國科會補助計畫衍生研發成果推廣資料表

日期:2012/01/30

國科會補助計畫	計畫名稱: 應用非線性時變模式之大型風力機用增速行星齒輪箱承受變動負載之動態響應分析
	計畫主持人: 黃國饒
	計畫編號: 99-2221-E-216-003- 學門領域: 機構與傳動

無研發成果推廣資料

99 年度專題研究計畫研究成果彙整表

計畫主持人：黃國饒	計畫編號：99-2221-E-216-003-
計畫名稱：應用非線性時變模式之大型風力機用增速行星齒輪箱承受變動負載之動態響應分析	

成果項目			量化			單位	備註（質化說明：如數個計畫共同成果、成果列為該期刊之封面故事...等）
			實際已達成數（被接受或已發表）	預期總達成數(含實際已達成數)	本計畫實際貢獻百分比		
國內	論文著作	期刊論文	0	0	100%	篇	
		研究報告/技術報告	1	0	100%		
		研討會論文	2	2	100%		
		專書	0	0	100%		
	專利	申請中件數	0	0	100%	件	
		已獲得件數	0	0	100%		
	技術移轉	件數	0	0	100%	件	
		權利金	0	0	100%	千元	
	參與計畫人力（本國籍）	碩士生	2	2	100%	人次	
		博士生	0	0	100%		
		博士後研究員	0	0	100%		
		專任助理	0	0	100%		
國外	論文著作	期刊論文	0	1	100%	篇	
		研究報告/技術報告	0	0	100%		
		研討會論文	2	2	100%		1. The First IFToMM Asian Conference on Mechanism and Machine Science 2. 2011 ASME International Design Engineering Technical Conferences (DETC 2011)
		專書	0	0	100%	章/本	
	專利	申請中件數	0	0	100%	件	
		已獲得件數	0	0	100%		
	技術移轉	件數	0	0	100%	件	
		權利金	0	0	100%	千元	
	參與計畫人力（外國籍）	碩士生	0	0	100%	人次	
		博士生	0	0	100%		
		博士後研究員	0	0	100%		

		專任助理	0	0	100%		
其他成果 (無法以量化表達之成果如辦理學術活動、獲得獎項、重要國際合作、研究成果國際影響力及其他協助產業技術發展之具體效益事項等，請以文字敘述填列。)		與大型風力機之增速齒輪箱產業聯繫配合					

	成果項目	量化	名稱或內容性質簡述
科教處計畫加填項目	測驗工具(含質性與量性)	0	
	課程/模組	0	
	電腦及網路系統或工具	0	
	教材	0	
	舉辦之活動/競賽	0	
	研討會/工作坊	0	
	電子報、網站	0	
	計畫成果推廣之參與（閱聽）人數	0	

國科會補助專題研究計畫成果報告自評表

請就研究內容與原計畫相符程度、達成預期目標情況、研究成果之學術或應用價值（簡要敘述成果所代表之意義、價值、影響或進一步發展之可能性）、是否適合在學術期刊發表或申請專利、主要發現或其他有關價值等，作一綜合評估。

1. 請就研究內容與原計畫相符程度、達成預期目標情況作一綜合評估

■達成目標

□未達成目標（請說明，以 100 字為限）

□實驗失敗

□因故實驗中斷

□其他原因

說明：

2. 研究成果在學術期刊發表或申請專利等情形：

論文：□已發表 □未發表之文稿 ■撰寫中 □無

專利：□已獲得 □申請中 ■無

技轉：□已技轉 ■洽談中 □無

其他：(以 100 字為限)

本計畫研究計畫成果已發表三篇研討會論文:

1. 大型風力機用多階齒輪傳動系統之特性分析，2010 臺灣風能學術研討會，澎湖。

2. 曲齒聯軸器之電腦輔助設計與實體建模，第 14 屆全國機構與機器設計學術研討會論文集，桃園。

3. A finite element investigation to modal and dynamic behaviors of planetary gearings concerning the effect of bearing and carrier stiffness,' DETC 2011, Las Vegas, USA.(EI)

3. 請依學術成就、技術創新、社會影響等方面，評估研究成果之學術或應用價值（簡要敘述成果所代表之意義、價值、影響或進一步發展之可能性）（以 500 字為限）

本研究應用等效離散模式和有限元素方法分析行星齒輪系統動態特性，完成可用於廣泛設計參數之內/外螺旋齒輪對之非線性時變等效嚙合剛度計算，也推導出可包含剛體運動影響單級螺旋行星齒輪系運動方程式，並考慮包含軸承、輸出入軸、轉速及變動負載之影響，可分析風場與操作條件等變動負載之單級齒輪系統的動態特性，探討齒輪應力、軸承負載與模態特性，獲得單階行星式螺旋齒輪箱包括起動、剎車、停機之動態特性分析技術與成果，若繼續推展可以完成國內風力機用增速行星齒輪箱以及各種高階齒輪傳動系統的設計分析技術建立。並整理結果如下：

1. 獲得應用非線性時變模式之螺旋行星式齒輪箱承受變動負載下動態特性分析技術。

2. 獲得可包含眾多齒輪設計參數的內外螺旋齒輪對的時變等效剛性模式、包括模數、齒數、螺旋角、移位量、背隙等。

3.有效率的分析非線性時變動態，並探討起動、加減速、剎車等運轉條件與負載變動下之動態特性。

4. 技術突破可協助國內風力機行星齒輪箱與各種高階齒輪傳動系統設計分析技術建立。
5.本計畫研發學術水準與工程應用皆與國際研究相當，部分成果已發表三篇研討會論文，並預計於 101 年 4 月投稿於國際期刊 ASME Journal of Mechanical Design。